Computational Technique and Performance of Transient Inundation Model for Rivers – 2 Dimensional (TRIM2RD): A Depth-Averaged Two-Dimensional Flow Model

Open-File Report 03-371

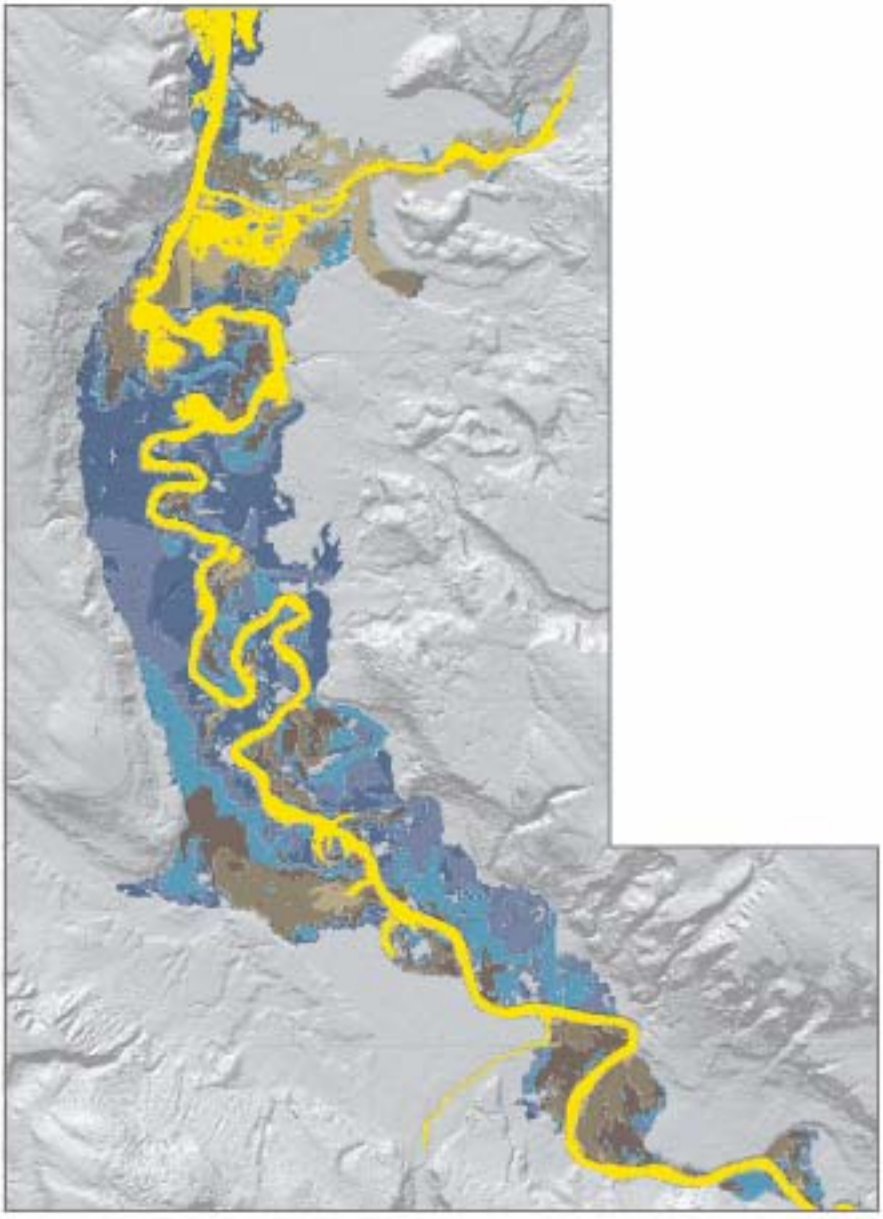

U.S. DEPARTMENT OF THE INTERIOR
U.S. GEOLOGICAL SURVEY

USGS
science for a changing world

Computational Technique and Performance of Transient Inundation Model for Rivers—2 Dimensional (TRIM2RD): A Depth-Averaged Two-Dimensional Flow Model

By Janice M. Fulford

U.S. GEOLOGICAL SURVEY

OPEN–FILE REPORT 03-371

Tacoma, Washington

2003

U.S. DEPARTMENT OF THE INTERIOR
GALE A. NORTON, Secretary

U.S. GEOLOGICAL SURVEY
Charles G. Groat, Director

Any use of trade, firm, or product names is for descriptive purposes only and does not imply endorsement by the U.S. Government

---

For additional information write to:

Director, Washington Water Science Center
U.S. Geological Survey
1201 Pacific Avenue – Suite 600
Tacoma, Washington 98402
http://wa.water.usgs.gov

Copies of this report can be purchased from:

U.S. Geological Survey
Information Services
Building 810
Box 25286, Federal Center
Denver, CO 80225-0286

Table of Contents

Figures

Tables

Conversion Factors and Abbreviations

Multiply	By	To obtain
Length		
centimeter (cm)	0.3937	inch (in.)
meter (m)	3.281	foot (ft)
kilometer (km)	0.6214	mile (mi)
kilometer (km)	0.5400	mile, nautical (nmi)
Flow rate		
square meter per second (m^2/s)	10.76	Square foot per second (ft^2/d)
meter per second (m/s)	3.281	foot per second (ft/s)

COMPUTATIONAL TECHNIQUE AND PERFORMANCE OF TRANSIENT INUNDATION MODEL FOR RIVERS — 2 DIMENSIONAL (TRIMR2D): A DEPTH–AVERAGED TWO–DIMENSIONAL FLOW MODEL

By Janice M. Fulford

ABSTRACT

A numerical computer model, Transient Inundation Model for Rivers – 2 Dimensional (TrimR2D), that solves the two-dimensional depth-averaged flow equations is documented and discussed. The model uses a semi-implicit, semi-Lagrangian finite-difference method. It is a variant of the Trim model and has been used successfully in estuarine environments such as San Francisco Bay. The abilities of the model are documented for three scenarios: uniform depth flows, laboratory dam-break flows, and large-scale riverine flows. The model can start computations from a “dry” bed and converge to accurate solutions. Inflows are expressed as source terms, which limits the use of the model to sufficiently long reaches where the flow reaches equilibrium with the channel. The data sets used by the investigation demonstrate that the model accurately propagates flood waves through long river reaches and simulates dam breaks with abrupt water-surface changes.

INTRODUCTION

River flooding is a significant natural hazard. The 1993 Mississippi River flood caused losses worth 15 to 20 billion dollars and 48 deaths (Perry, 2000). Flood-response planners need flow measurements, estimates of inundated areas, and prediction of river flows throughout a river valley to plan remediation actions and public-safety responses. Usually, measurements of river discharge and stage and predictions of flood stage from runoff calculations are limited to a few locations in the river valley. Stage and flow predictions at a few additional locations typically are done with one-dimensional storage-routing models. These models do not adequately account for inertia or backwater effects. The depth and extent of inundation at other locations in the river valley must be approximated from the available data, either measured or predicted. The paucity of flood information can hamper mitigation and public-safety decisions.

Methods are available that can increase the amount of flood information available for decision-making. Numerical computer models that solve the shallow-water equations can be used to simulate flow and provide information at locations where no measurements are available. Two-dimensional depth-averaged models can be used to predict flood inundation throughout the river valley from forecast flows at point locations (Bates and DeRoo, 2000).

The U. S. Geological Survey (USGS) is investigating a numerical flow model, Transient Inundation Model for Rivers - 2 Dimensional (TrimR2D), for providing near-real-time flood information on the Internet. The model will be used to calculate the extent of flood inundation and flow features such as stage and velocity distributions from forecast flood hydrographs from the National Weather Service.

TrimR2D is a two-dimensional numerical flow model that is extensively based on the Trim model (Casulli, 1990; Cheng and others, 1993) written by V. Casulli of the University of Trento, Italy. The Trim model initially was developed for estuarine applications and used to simulate flows in San Francisco Bay (Cheng and others, 1993). The outstanding numerical stability characteristics of the Trim2D model made its adaptation to riverine modelling appealing. Trim2D was adapted to river systems by modifying the input and output routines and by modifying boundary conditions for the needs of river modeling. The model has been used to model flows in steep river systems (Ostenaa and others, 1999).

Some work using the model has been published. Test cases confirming the lack of spurious modes and the second-order convergence rate for uniform grid refinement were performed by Walters and Denlinger (1999). However, no confirmation of model results with measured data was published for the river simulation described by Walters and Denlinger (1999). Examples comparing results from the TrimR2D parent code with measurements have been published for oceanographic conditions (Cheng and others, 1993).

Purpose and Scope

This report describes the computational technique and demonstrates the performance in river systems of the TrimR2D computational flow model. The description of the computational technique includes a presentation of the governing equations and the numerical solution used to solve the governing equations. Model performance for river applications is demonstrated and discussed for three types of scenarios: (1) uniform-depth flows, (2) laboratory dam-break flows, and (3) large-scale riverine flows. The format of model input and output files is documented in the appendix.

Acknowledgments

The assistance of Dr. Roy Walters (U.S. Geological Survey, retired) is greatly appreciated. His advice and interest in the study has made this report possible.

GOVERNING EQUATIONS

The governing equations for TrimR2D are commonly known as the shallow-water equations. The shallow-water equations describe two-dimensional, depth-averaged, unsteady flow and are based on the conservation of mass and momentum. The equations assume that water is incompressible and that pressure distribution is hydrostatic. Density is constant throughout the water column and vertical velocities are considered small relative to the horizontal velocities. In differential form, the governing equations of continuity (eq. 1) and momentum (eqs. 2 and 3) conservation that are solved by TrimR2D have the form

$$\frac{\partial \zeta}{\partial t} + \frac{\partial\left[(h+\zeta)u\right]}{\partial x} + \frac{\partial\left[(h+\zeta)v\right]}{\partial y} = 0 \quad , \tag{1}$$

$$\frac{\partial u}{\partial t} + u\frac{\partial u}{\partial x} + v\frac{\partial u}{\partial y} = -g\frac{\partial \zeta}{\partial x} + \frac{1}{\rho\left(h+\zeta\right)}\left(\tau_x^w - \tau_x^b\right) + A_h\nabla^2 u + fv \quad , \tag{2}$$

and

$$\frac{\partial v}{\partial t} + u\frac{\partial v}{\partial x} + v\frac{\partial v}{\partial y} = -g\frac{\partial \zeta}{\partial y} + \frac{1}{\rho\left(h+\zeta\right)}\left(\tau_y^w - \tau_y^b\right) + A_h\nabla^2 v - fu \quad , \tag{3}$$

where t is time; $u(x,y,t)$ and $v(x,y,t)$ are the depth-averaged velocity components in the x- and y-axis directions in the horizontal plane, respectively; $\zeta(x,y,t)$ is the water-surface elevation measured from the vertical datum; $h(x,y)$ is the depth measured from the vertical datum; g is the acceleration of gravity; f is the Coriolis parameter; τ_x^b and τ_y^b are the bottom-stress terms; τ_x^w and τ_y^ω are the wind-stress terms in the x- and y-axis directions; $\nabla = \vec{i}\,\partial/\partial x + \vec{j}\,\partial/\partial y$ is a vector operator in the horizontal x-y plane; and A_h is the horizontal eddy viscosity. The vertical datum is arbitrary and is selected to minimize numerical truncation errors. Usually, for oceanographic applications, mean sea level is the vertical datum. For river applications, the approximate outflow elevation is the vertical datum. Figure 1 illustrates the relation between the vertical datum and variables that represent depth and water-surface elevation. The water depth, H, is equal to $(h+\zeta)$. The depth, $h(x,y)$, measured from the vertical datum, is positive in the down direction and negative in the up direction. The depth (or distance to the land surface) is elevation of the topography referenced to the vertical datum. The water-surface elevation, $\zeta(x,y,t)$, measured from the vertical datum, is positive in the up direction and negative in the down direction.

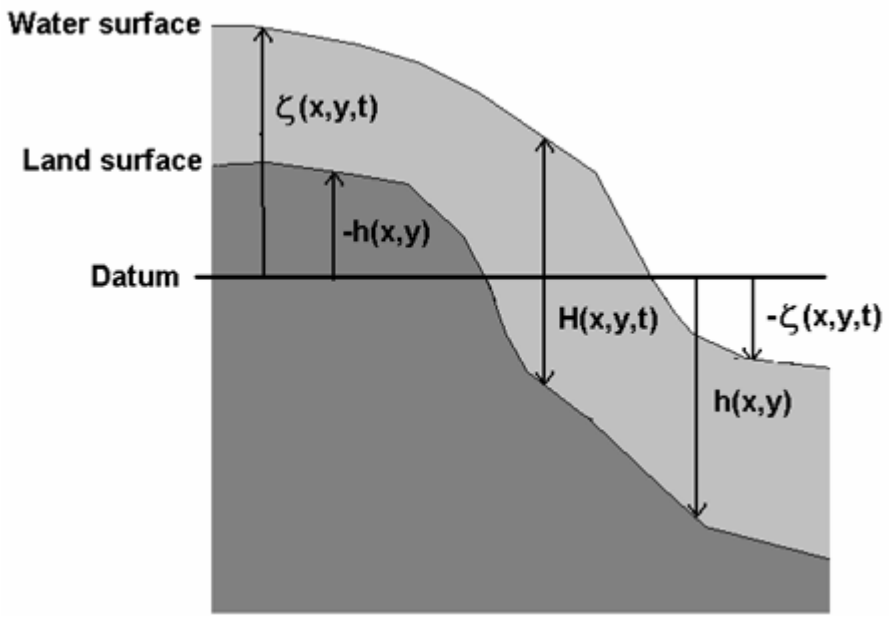

Figure 1. Relation between vertical datum and variables representing depth and water-surface elevation

The bottom-stress terms are formulated using a Manning-Chezy type expression as

$$\frac{1}{\rho(h+\zeta)}\tau_x^b = \gamma u \qquad \textbf{(4)}$$

and

$$\frac{1}{\rho(h+\zeta)}\tau_x^b = \gamma v \ , \qquad \textbf{(5)}$$

where

$$\gamma = \frac{g\sqrt{u^2+v^2}}{C^2(h+\zeta)} \qquad \textbf{(6)}$$

is the bed friction factor.

C is the Chezy coefficient. Manning's coefficient in metric units is related to Chezy coefficient by

$$n = \frac{(h+\zeta)^{1/6}}{C} \ . \qquad \textbf{(7)}$$

NUMERICAL SOLUTION

The shallow-water equations are not amenable to direct solution and require that the continuous derivatives in the equations be approximated by finite-difference techniques. Finite-difference techniques solve the governing equations for a finite number of locations in space and time. The techniques require the subdivision of the application domain into a mesh (or grid) with a finite number of node points.

The numerical solution of the governing equations uses a semi-implicit finite-difference method that approximates the advective terms of the momentum equations with a Lagrangian formulation. Simulation of the topography wetting and drying is permitted by the solution algorithm. The following is a brief overview of the numerical method, wetting and drying computations, boundary conditions, and roughness parameters. Details on the derivation and stability of the numerical technique are documented in Casulli (1990) and Casulli and Cattani (1994).

Numerical Method

The equations are spatially discretized as a staggered rectangular mesh that consists of square computational cells with length Δx and width Δy ($\Delta x=\Delta y$). Figure 2 illustrates the computational mesh used in the spatial discretization. Water-surface elevation, ζ, is defined at cell centers with an index of (*i,j*), and velocities *u,v* are defined at the middle of cell sides with an index of (*i+1/2*,*j+1/2*). The x-axis velocities, $u_{i+\frac{1}{2},j}$ and $u_{i-\frac{1}{2},j}$, are defined at the right and left sides of the cell, and the y-axis velocities, $v_{i,j+\frac{1}{2}}$ and $v_{i,j-\frac{1}{2}}$, are defined at the upper and lower sides of the cell. An arithmetic average of the surrounding values is used for variables not defined at a spatial location.

Depth or land topography, *h*, is defined at the velocity locations. However, land topography is input to TrimR2D at node and half-node mesh locations. The resulting topography mesh has a resolution that is twice that of the computational mesh. The higher resolution of the topography mesh eliminates the need for users to construct a staggered topography mesh and eliminates a potential source of user error.

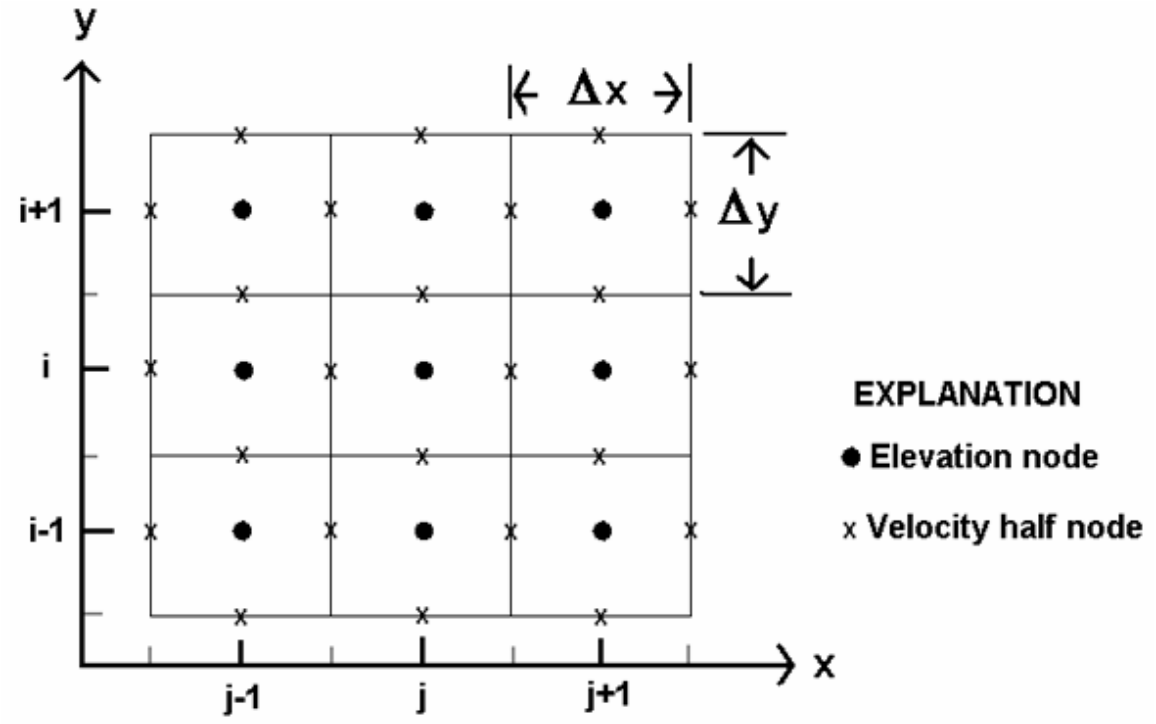

Figure 2. Computational mesh used in spatial discretization

The temporal discretization is a mixture of explicit and implicit methods. The gradients of water-surface elevation ($g\frac{\partial \zeta}{\partial x}$, $g\frac{\partial \zeta}{\partial y}$) in the momentum equations (eq. 2 and 3) and the velocity divergence ($\frac{\partial u}{\partial x}$, $\frac{\partial v}{\partial y}$) in the continuity equation (eq. 1) are discretized semi-implicitly to remove the stability constraint for gravity waves. The velocity part of the friction terms (γu , γv) in the momentum equations is discretized implicitly. The γ parts of the friction terms in the momentum equations and the water depth terms ($h+z$) in the continuity equation are discretized explicitly.

The advective terms ($\frac{\partial v}{\partial t} + u\frac{\partial v}{\partial x} + v\frac{\partial v}{\partial y}$, $\frac{\partial u}{\partial t} + u\frac{\partial u}{\partial x} + v\frac{\partial u}{\partial y}$) in the momentum equations are expressed as a substantial (or material) derivative, *D/Dt*, resulting in

$$\frac{Du}{Dt} = -g\frac{\partial \zeta}{\partial x} + \frac{1}{\rho(h+\zeta)}\left(\tau_x^w - \tau_x^b\right) + A_h\nabla^2 u + fv \quad \textbf{(8)}$$

and

$$\frac{Dv}{Dt} = -g\frac{\partial \zeta}{\partial y} + \frac{1}{\rho(h+\zeta)}\left(\tau_y^w - \tau_y^b\right) + A_h\nabla^2 v - fu \quad . \quad \textbf{(9)}$$

Equations (8) and (9) are discretized in time with a forward difference operator.

The semi-implicit discretization of equations (1), (8), and (9) have the form

$$\begin{aligned}\zeta_{i,j}^{k+1} = \zeta_{i,j}^k &- \theta\frac{\Delta t}{\Delta x}\left[\left(h_{i+\frac{1}{2},j} + \max\left(\zeta_{i,j}^k, \zeta_{i+1,j}^k\right)\right)u_{i+\frac{1}{2},j}^{k+1} - \left(h_{i-\frac{1}{2},j} + \max\left(\zeta_{i,j}^k, \zeta_{i-1,j}^k\right)\right)u_{i-\frac{1}{2},j}^{k+1}\right] \\ &- \theta\frac{\Delta t}{\Delta y}\left[\left(h_{i,j+\frac{1}{2}} + \max\left(\zeta_{i,j}^k, \zeta_{i,j+1}^k\right)\right)v_{i,j+\frac{1}{2}}^{k+1} - \left(h_{i,j-\frac{1}{2}} + \max\left(\zeta_{i,j}^k, \zeta_{i,j-1}^k\right)\right)v_{i,j-\frac{1}{2}}^{k+1}\right] \\ &- (1-\theta)\frac{\Delta t}{\Delta x}\left[\left(h_{i+\frac{1}{2},j} + \max\left(\zeta_{i,j}^k, \zeta_{i+1,j}^k\right)\right)u_{i+\frac{1}{2},j}^{k} - \left(h_{i-\frac{1}{2},j} + \max\left(\zeta_{i,j}^k, \zeta_{i-1,j}^k\right)\right)u_{i-\frac{1}{2},j}^{k}\right] \\ &- (1-\theta)\frac{\Delta t}{\Delta y}\left[\left(h_{i,j+\frac{1}{2}} + \max\left(\zeta_{i,j}^k, \zeta_{i,j+1}^k\right)\right)v_{i,j+\frac{1}{2}}^{k+1} - \left(h_{i,j-\frac{1}{2}} + \max\left(\zeta_{i,j}^k, \zeta_{i,j-1}^k\right)\right)v_{i,j-\frac{1}{2}}^{k+1}\right] \quad \textbf{(10)}\end{aligned}$$

$$\begin{aligned}u_{i+\frac{1}{2},j}^{k+1} = Iu_{i+\frac{1}{2},j}^k &- \theta g\frac{\Delta t}{\Delta x}\left(\zeta_{i+1,j}^{k+1} - \zeta_{i,j}^{k+1}\right) - \Delta t\left(\gamma_{i+\frac{1}{2},j}^k u_{i+\frac{1}{2},j}^{k+1} - \left(fv + \frac{1}{\rho(h+\zeta)}\tau_x^w\right)_{i+\frac{1}{2},j}^k\right) \\ &- (1-\theta)g\frac{\Delta t}{\Delta x}\left(\zeta_{i+1,j}^k - \zeta_{i,j}^k\right) \quad \textbf{(11)}\end{aligned}$$

$$\begin{aligned}v_{i,j+\frac{1}{2}}^{k+1} = Iv_{i,j+\frac{1}{2}}^k &- \theta g\frac{\Delta t}{\Delta y}\left(\zeta_{i,j+1}^{k+1} - \zeta_{i,j}^{k+1}\right) - \Delta t\left(\gamma_{i,j+\frac{1}{2}}^k v_{i,j+\frac{1}{2}}^{k+1} - \left(\frac{1}{\rho(h+\zeta)}\tau_y^w - fv\right)_{i,j+\frac{1}{2}}^k\right) \\ &- (1-\theta)g\frac{\Delta t}{\Delta y}\left(\zeta_{i+1,j}^k - \zeta_{i,j}^k\right) \quad . \quad \textbf{(12)}\end{aligned}$$

In equation 10, terms similar to $\max\left(\zeta_{i,j}^k, \zeta_{i+1,j}^k\right)$ denote that the maximum value between the parentheses is selected and used in the equation. The variable θ is a temporal difference operator. *I* is a nonlinear finite-difference operator that only contains terms at the previous time step. The eddy viscosity terms in the momentum equations have been neglected for the sake of simplicity, but are included in the actual formulation used by TrimR2D with an explicit discretization and hence a weak stability constraint.

The momentum equations (11) and (12) are substituted into the continuity equation (10). The resulting equation is solved for water-surface elevation at the new time step and has the form

$$\zeta_{i,j}^{k+1} + g\theta^2 \frac{\Delta t^2}{\Delta x^2}\left[\frac{\overline{\zeta}_{i+½,j}^{k} + h_{i+½,j}}{1+\gamma_{i+½,j}^{k}\Delta t}\left(\zeta_{i,j}^{k+1} - \zeta_{i+1,j}^{k+1}\right) + \frac{\overline{\zeta}_{i-½,j}^{k} + h_{i-½,j}}{1+\gamma_{i-½,j}^{k}\Delta t}\left(\zeta_{i,j}^{k+1} - \zeta_{i-1,j}^{k+1}\right)\right]$$

$$+ g\theta^2 \frac{\Delta t^2}{\Delta y^2}\left[\frac{\overline{\zeta}_{i,j+½}^{k} + h_{i,j+½}}{1+\gamma_{i,j+½}^{k}\Delta t}\left(\zeta_{i,j}^{k+1} - \zeta_{i,j+1}^{k+1}\right) + \frac{\overline{\zeta}_{i,j-½}^{k} + h_{i,j-½}}{1+\gamma_{i,j-½}^{k}\Delta t}\left(\zeta_{i,j}^{k+1} - \zeta_{i,j-1}^{k+1}\right)\right]$$

$$= \zeta_{i,j}^{k} - \frac{\Delta t}{\Delta x} u_{i+½,j}^{k}\left(\overline{\zeta}_{i+½,j}^{k} + h_{i+½,j}\right)\left[1+\theta\left(1+\frac{I}{\left(1+\gamma_{i+½,j}^{k}\Delta t\right)}\right)\right]$$

$$+ \frac{\Delta t}{\Delta x} u_{i-½,j}^{k}\left(\overline{\zeta}_{i-½,j}^{k} + h_{i-½,j}\right)\left[1+\theta\left(1+\frac{I}{1+\gamma_{i-½,j}^{k}\Delta t}\right)\right]$$

$$- g\theta(1-\theta)\left(\frac{\Delta t}{\Delta x}\right)^2\left\{\frac{\left(\overline{\zeta}_{i+½,j}^{k} + h_{i+½,j}\right)}{\left(1+\gamma_{i+½,j}^{k}\Delta t\right)}\left(\zeta_{i+1,j}^{k} - \zeta_{i,j}^{k}\right) - \frac{\left(\overline{\zeta}_{i-½,j}^{k} + h_{i-½,j}\right)}{\left(1+\gamma_{i-½,j}^{k}\Delta t\right)}\left(\zeta_{i-1,j}^{k} - \zeta_{i,j}^{k}\right)\right\}$$

$$- \frac{\Delta t}{\Delta y} u_{i,j+½}^{k}\left(\overline{\zeta}_{i,j+½}^{k} + h_{i,j+½}\right)\left[1+\theta\left(1+\frac{I}{1+\gamma_{i,j+½}^{k}\Delta t}\right)\right]$$

$$+ \frac{\Delta t}{\Delta y} u_{i,j-½}^{k}\left(\overline{\zeta}_{i,j-½}^{k} + h_{i,j-½}\right)\left[1+\theta\left(1+\frac{I}{1+\gamma_{i,j-½}^{k}\Delta t}\right)\right]$$

$$- g\theta(1-\theta)\left(\frac{\Delta t}{\Delta y}\right)^2\left\{\frac{\left(\overline{\zeta}_{i,j+½}^{k} + h_{i,j+½}\right)}{\left(1+\gamma_{i,j+½}^{k}\Delta t\right)}\left(\zeta_{i,j+1}^{k} - \zeta_{i,j}^{k}\right) - \frac{\left(\overline{\zeta}_{i,j-½}^{k} + h_{i,j-½}\right)}{\left(1+\gamma_{i,j-½}^{k}\Delta t\right)}\left(\zeta_{i,j-1}^{k} - \zeta_{i,j}^{k}\right)\right\} \quad \textbf{(13)}$$

where $\overline{\zeta}^{k}$ is the average water elevation over a mid-side node. The Coriolis and wind terms have been neglected in equation (13) to simplify the presentation of the discretized equations. These terms are included in the formulation used by the model, however they are not needed for river applications. Equation (13) is a linear penta-diagonal system of equations. The resulting matrix is positive definite and has a unique solution when

$$\left(\zeta_{i\pm½,j}^{k} + h_{i\pm½,j}\right) \geq 0 \quad \textbf{AND} \quad \left(\zeta_{i,j\pm½}^{k} + h_{i,j\pm½}\right) \geq 0 \ .$$

The matrix is solved using a conjugate-gradient method that is suitable for vector computations.

In order to obtain an unconditionally stable and relatively accurate form for *I*, an Eulerian-Lagrangian approximation is used. The substantial derivative of a general variable, *w*, is

$$\frac{Dw}{Dt} = \frac{\partial w}{\partial t} + u\frac{\partial w}{\partial t} + v\frac{\partial w}{\partial t}\ , \tag{14}$$

where *D/Dt* represents the time rate of change along a streamline defined by

$$\frac{dx}{dt} = u\ , \frac{dy}{dt} = v\ . \tag{15}$$

As previously shown in equations 11 and 12, the substantial derivative can be discretized in time as

$$\frac{Dw}{Dt} \approx \frac{w_{i,j}^{k+1} - Iw_{i,j}^{k}}{\Delta t}\ . \tag{16}$$

The term $Iw_{i,j}^{k}$ is the value of *w* at time t_k located at (i-a,j-b) which is convected in the grid in an elapsed time Δt. Thus,

$$\frac{Dw}{Dt} \approx \frac{w_{i,j}^{k+1} - w_{i-a,j-b}^{k}}{\Delta t}\ , \tag{17}$$

where

$$a = u\frac{\Delta t}{\Delta x}\ , b = v\frac{\Delta t}{\Delta y}\ . \tag{18}$$

Because *a* and *b* are not usually integers, bilinear interpolation is used to approximate the current value of *w* at t_k. Letting $a = n+p$ and $b=m+q$ where *n* and *m* are integers and $0 \le p < 1$, and $0 \le q < 1$, $Iw_{i,j}^{k}$ is approximated by

$$Iw_{i,j}^{k} = w_{i-a,j-b}^{k} = (1-p)\left[(1-q)\,w_{i-n,j-m}^{k} + q w_{i-n,j-m-1}^{k}\right] + p\left[(1-q)\,w_{i-n-1,j-m}^{k} + q w_{i-n-1,j-m-1}^{k}\right]. \tag{19}$$

The computational module for TrimR2D is diagrammed in figure 3. It illustrates how equation 19 includes terms from cells that are not necessarily adjacent to the computational node at (i,j).

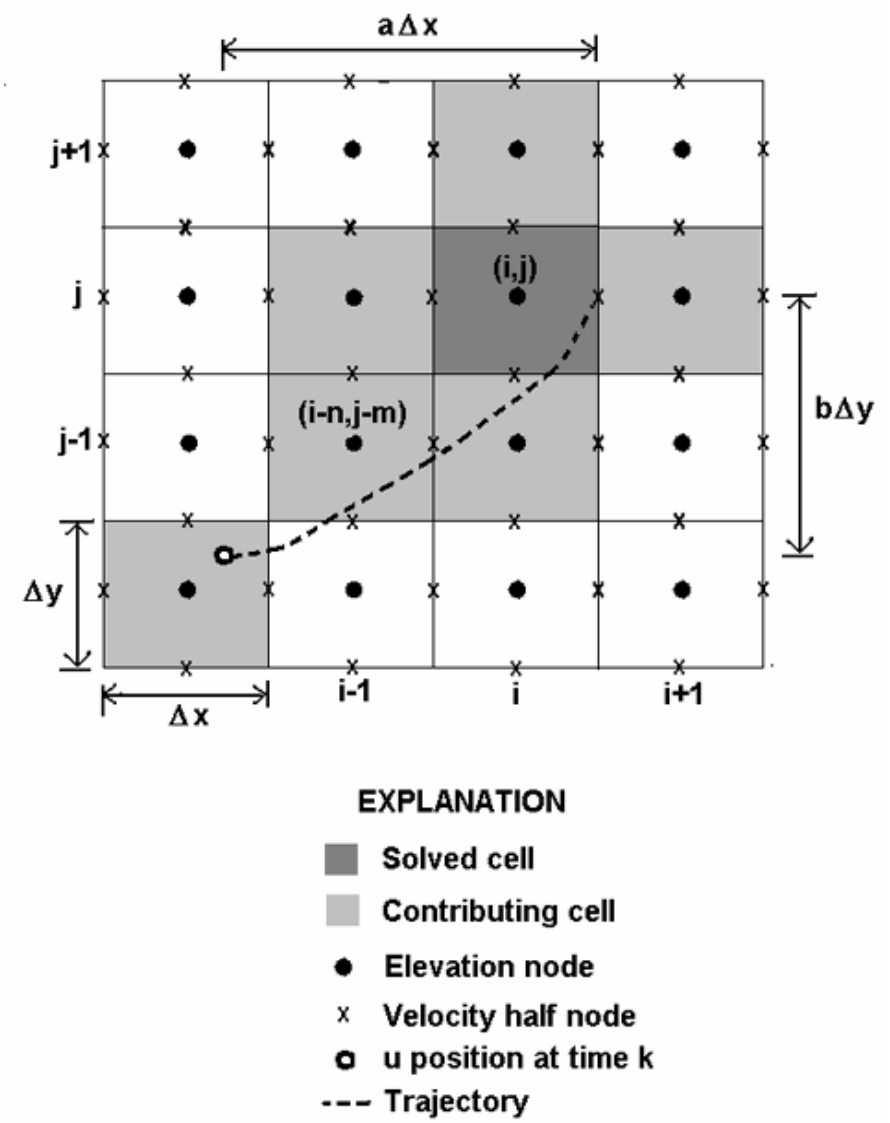

Figure 3. Computational module for TrimR2D, showing how terms from non-adjacent cells are included in the computational node at (i,j)

Because u and v are not usually constants, the correct value of a and b is found from numerically integrating the ordinary differential equations in equation (17) from t_0 to t_1 by the Euler method (Conte and DeBoor, 1980). The time step, Δt, is divided for the integration method into N equal time parts, so that $\Delta t' = \Delta t/N$. The time subdivision is restricted to be

$$\Delta t' \leq \min\left[\frac{\Delta x}{\max_{i,j}\left|u^{k}_{i+\frac{1}{2},j}\right|}, \frac{\Delta y}{\max_{i,j}\left|v^{k}_{i,j+\frac{1}{2}}\right|}\right] . \quad \textbf{(20)}$$

This restriction prevents the approximated streamlines from crossing solid boundaries. This condition is not required for the stability of the method, but improves the accuracy.

The overall mesh shape for any application of TrimR2D is a rectangle. However, computation does not necessarily occur for every cell in the mesh. The model ignores the computation of cells with topography higher than a user-defined elevation. This reduces the solution matrix size and permits some flexibility in representing areas that are permanently dry.

Wetting and Drying

The discretized equation (13) inherently permits wetting and drying of cells without using complicated bookkeeping procedures. If the water elevation in a wet adjacent cell is higher than the topography at the "half" node, flow will enter the cell from the adjacent cell. To prevent the introduction of non-physical, negative values of total flow depth, H is limited to be max (0, $h+\zeta$). When H is zero, the respective bed friction factor, γ, is assumed large.

Boundary Conditions

Two types of boundary conditions are available in the model, an external water-surface elevation boundary and an internal source. Both boundary conditions are time varying and exploit the properties of the discretized equation (13). The inclusion of these boundary conditions allows the solution matrix to maintain a penta-diagonal form with no off-diagonal terms.

The external water-surface elevation boundary sets a spatially uniform water elevation on the perimeter of the model mesh. To apply the external water-surface boundary, the model adds boundary cells to the perimeter of the user-defined mesh. In the boundary cells the water-surface elevation can be specified by either a time series or a harmonic function. Flow from the boundary cells occurs when the topography and water elevation of an abutting cell are lower than the water-surface elevation in the boundary cells. Flow out of the model occurs when the water-surface elevation in the boundary cells is less than the water-surface elevation in an abutting wet cell.

The internal boundary condition, point sources, is the only method in the model available to add flow. Flow is introduced to the model mesh by the addition of a source term to the continuity equation

$$\frac{\partial \zeta}{\partial t} + \frac{\partial[(h+\zeta)u]}{\partial x} + \frac{\partial[(h+\zeta)v]}{\partial y} = q \quad , \qquad \textbf{(21)}$$

where q is the discharge. The source term is expressed as $q_{i,j}^{k+1}$ on the right side of the discretized equation for water-surface elevation (eq. 13). The location of each source is specified by individual cell locations in the mesh. Flow for a cell containing a source (source cell) is specified by a time series of discharge values. Flow out of the source cell follows the rules for wetting and drying. Thus, when the water elevation in a source cell is higher than the water elevation and topography in an adjacent cell, flow out of the source cell occurs. The method for adding flow is analogous to a spring flowing

vertically into a water body. The method does not account for the momentum effects that occur when water flows into a water body with a non-zero horizontal velocity. Hence, the simulation of river inflows with source terms will result in simulation errors near the location of the inflow.

The effect of the boundary conditions on the model is analogous to an island in an ocean. The external water-surface elevation boundary is the level of the ocean that surrounds the island. The sources are the springs on the island and they supply the river flow. A schematic of a simple mesh and the boundary conditions is shown in figure 4.

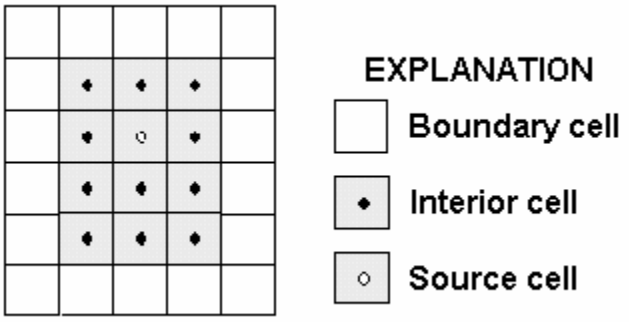

Figure 4. Schematic of a simple mesh and boundary conditions

Boundary cells are added by the program

Roughness Parameters

Roughness parameters for TrimR2D are Manning's *n*. Values of Manning's *n* can be varied as a function of flow depth, but cannot be varied as a function of location in the mesh. The model is not able to simulate flow patterns that result from spatially varying the roughness associated with differences in land use, soil, or vegetation types.

MODEL PERFORMANCE

This section demonstrates and discusses TrimR2D performance for typical river or open-channel flow type applications. No attempt is made to rigorously demonstrate spatial and temporal convergence of the solution by repeatedly increasing the resolution of the applications. It is assumed that the numerical scheme used and described in the previous sections is convergent (Cassulli and Cattani, 1994). Model simulations for three types of conditions are presented: (1) uniform-depth flows, where gravitational forces are in equilibrium with frictional forces; (2) laboratory-measured dam-break flows that are highly advective; and (3) large-scale (greater than a kilometer in length) river flows. Simulation results are compared with well-known channel resistance equations and with measured data as appropriate. The applications herein demonstrate the model's capability to simulate timing and magnitude of the water-surface elevation and peak water-surface

elevations for a limited number of locations within each application. Because of a lack of measured field data on flooded extent, no simulations demonstrate the performance of TrimR2D in determining flooded extent.

Uniform Depth Scenarios

Uniform depth is a concept familiar to hydraulic engineers. It occurs when a constant flow in a channel of uniform shape and slope is in equilibrium with gravitational forces. When equilibrium is reached, the flow depth is constant and the water-surface slope equals the slope of the channel. Simulating uniform depth demonstrates how the TrimR2D approximation of bed friction in riverine systems affects the model solution of the governing equations.

The uniform flow concept is expressed in the well-known engineering equation, Manning's equation (Chow, 1959)

$$Q = \frac{k}{n} A R^{2/3} S^{1/2} \quad , \tag{22}$$

where Q is the total discharge, n is the Manning's roughness coefficient, A is the cross-sectional area, R is the hydraulic radius, S is the channel slope (energy slope, equivalent to channel slope for uniform depth simulations), and k is a conversion factor that is 1 for meter-second units and 1.49 for feet-second units. The hydraulic radius is the cross-sectional area divided by the wetted perimeter of the channel cross section. It is approximately equal to the flow depth when a channel is wide relative to the flow depth. The equilibrium flow depth is called the uniform or "normal" depth and is different for each flow rate for a given channel. The Manning's equation, though somewhat empirical, has a long record of closely approximating uniform-flow depth in river systems. Originally determined by fitting measured data, the Manning's equation can be derived from the Navier-Stokes equations.

The uniform depth simulations were for a 1,000-meter-long straight channel with a 4-meter-wide rectangular cross section and a bed slope of 0.005. The topographic mesh (representing depth, h, in the governing equations) has half-meter cell resolution that result in 1-meter-sized computational cells. The computational mesh is 6 by 1,001 cells. Cell elevations on three sides of the computational mesh prevent flow through those sides for all the uniform depth simulations and restrict outflow to occur out one end of the channel.

Uniform depths were simulated for three scenarios (table 1) that have different discharges and roughnesses representing a wide range of channel materials. Boundary conditions, downstream water-surface elevation, and upstream source discharge are constant for all of the uniform-depth simulations. Discharges were computed using equation (22). However, the hydraulic radius used in the discharge equation was

computed by neglecting the contribution of the channel side walls to the wetted perimeter. This method of computation accounts for the omission by TrimR2D of friction losses due to vertical side walls.

At least two different downstream water-surface elevation boundary conditions were simulated for each scenario. For scenarios with subcritical flow conditions, backwater and drawdown water-surface profile curves were simulated. These water-surface profile curves are also referred to as M1 and M2 curves, respectively, by many hydraulic engineering texts (Chow, 1959). Backwater curves (M1) occur for subcritical flow when the downstream flow depth is larger than normal depth. Drawdown curves (M2) occur for subcritical flow when the downstream flow depth is smaller than normal depth. For both types of curves, the flow will converge toward normal depth in the upstream direction.

Table 1. Uniform depths for three scenarios representing a wide range of stream channel materials

Scenario	*Manning's roughness*	*Normal depth (meters)*	*Froude No.*	*Discharge (cubic meters per second)*
A	0.035	2.0	0.72	25.7
B	0.075	1.0	0.30	3.77
C	0.012	3.0	2.26	147

Simulations were for run times that usually allowed the computations to reach steady-state (equilibrium) flow conditions. All simulations began with a “dry” bed condition. Most two- and one-dimensional flow models cannot be started with all computational nodes having a zero flow depth. Usually, the user is required to create initial conditions for two-dimensional models by starting with a level water surface and for one-dimensional models by starting with a known water surface. TrimR2D does not require wet computational nodes to begin computations. However, because the simulations were started from a dry bed, a small time step was necessary. When the flow propagates over dry cells, the model can wet only the adjacent cell during a time step. For this case, the explicit terms in the discretized equation (eq. 13) dominate the first iterations of the solution and require time-step sizes similar to those used by fully explicit models.

Scenario A: Roughness of 0.035 With Uniform Depth of 2 Meters

The roughness for scenario A is typical of natural sand-and-gravel rivers. Water-surface profile simulations for outflow water depths of 2 m, 2.5 m, and 1.9 m are shown in figure 5. The outflow water depths of 2.5 m and 1.9 m represent a backwater (M1) curve and a drawdown (M2) curve (Chow, 1959), respectively. Scenario A simulations are for 10,000 0.1-second time steps and reach flow equilibrium before the simulation ends. Each simulated profile is for subcritical flow (F<1.0).

The computed uniform depth was 2.02 m for the three simulations and is 1 percent larger than the 2.00 m value computed by the Manning's equation. The depth is in equilibrium for the backwater curve (M1 curve) at about 357 m from the outflow end and for the drawdown curve (M2 curve) at about 147 m from the outflow end.

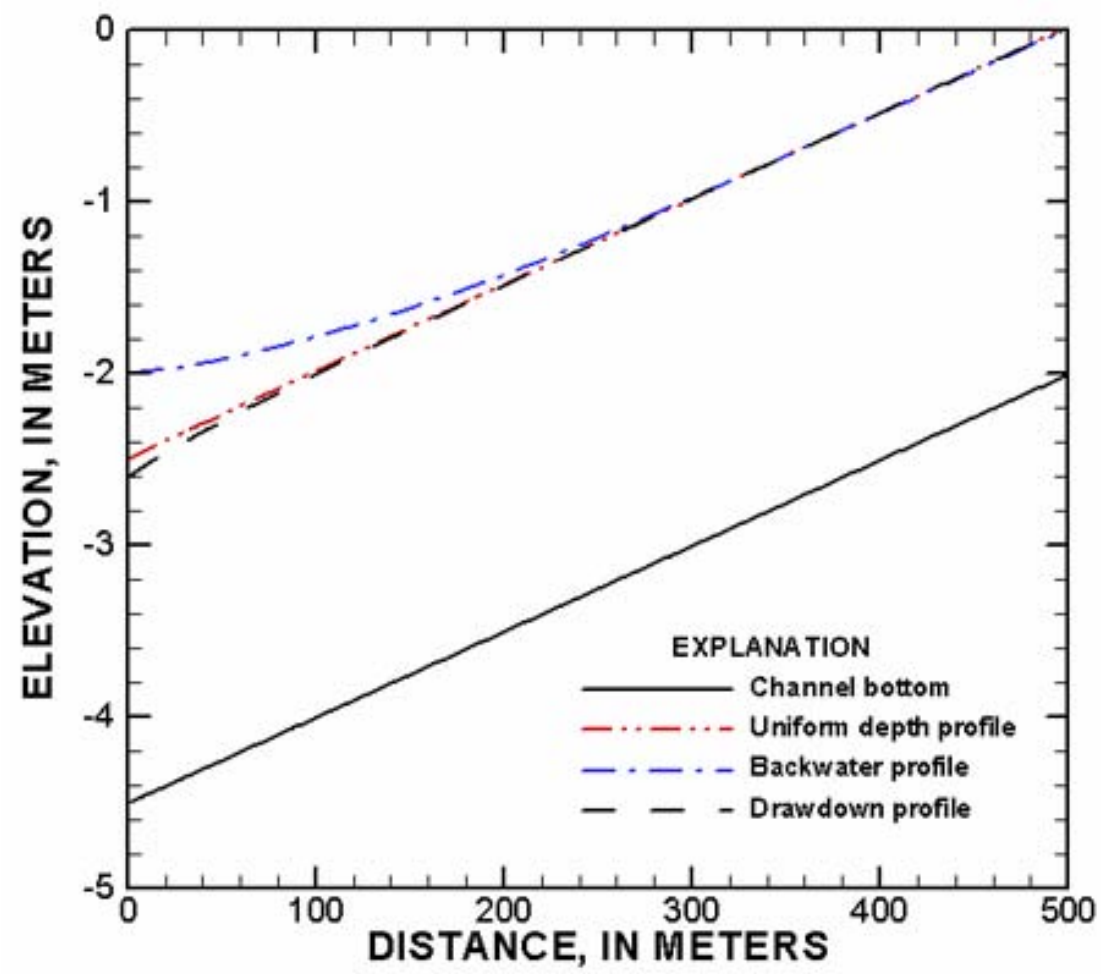

Figure 5. Simulated water-surface profiles for scenario A with a roughness of 0.035 and a uniform depth of 2 meters

Davidian (1984) presents an empirical equation for estimating the distance needed for a downstream water depth that is 125 percent of uniform depth to converge to uniform depth for subcritical-flow conditions (M1 curve):

$$\frac{LS_o}{Y_n} = 0.86 - 0.64F^2 \quad , \qquad \textbf{(23)}$$

where L is the required total reach length, S_o is the bed slope, Y_n is the uniform depth, and F is the Froude number. Agreement between Davidian's equation and the simulation results are good. For a water depth of 2.5 m at the outflow boundary (backwater simulation), the length of reach needed to converge within 3 percent of uniform depth is

210 m for equation (23), compared to 220 m for the simulation. The plot of flow depth versus channel distance in figure 6 illustrates the convergence of the simulation to uniform depth. The simulated backwater curve (M1 curve) slightly undershoots the depth before converging. The drawdown curve smoothly converges to the uniform depth.

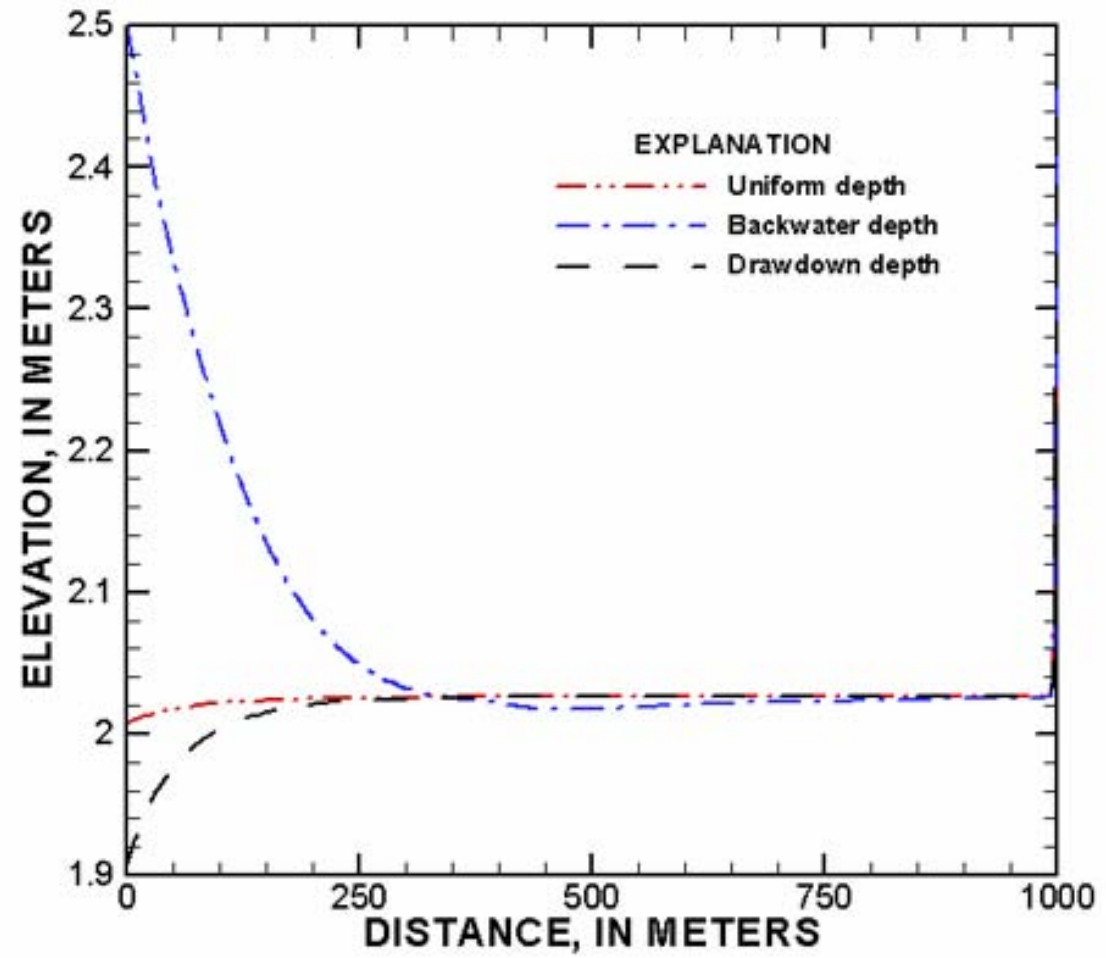

Figure 6. Simulated flow depth for scenario A with a roughness of 0.035 and a uniform depth of 2.0 meters

Scenario B: Roughness of 0.075 With Uniform Depth of 1Meter

The roughness for scenario B is representative of streams with dense vegetation or with large boulders and steep water-surface gradients. Water-surface profiles for outflow water depths of 1.5 m and 0.75 m are shown in figure 7. The outflow water depths of 1.5 m and 0.75 m represent a backwater (M1) curve and a drawdown (M2) curve, respectively. Subcritical flow occurs for each simulated profile ($F<1$). As in the previous scenario, scenario B simulations are for 10,000 0.1-second time steps and reach flow equilibrium before simulation ends.

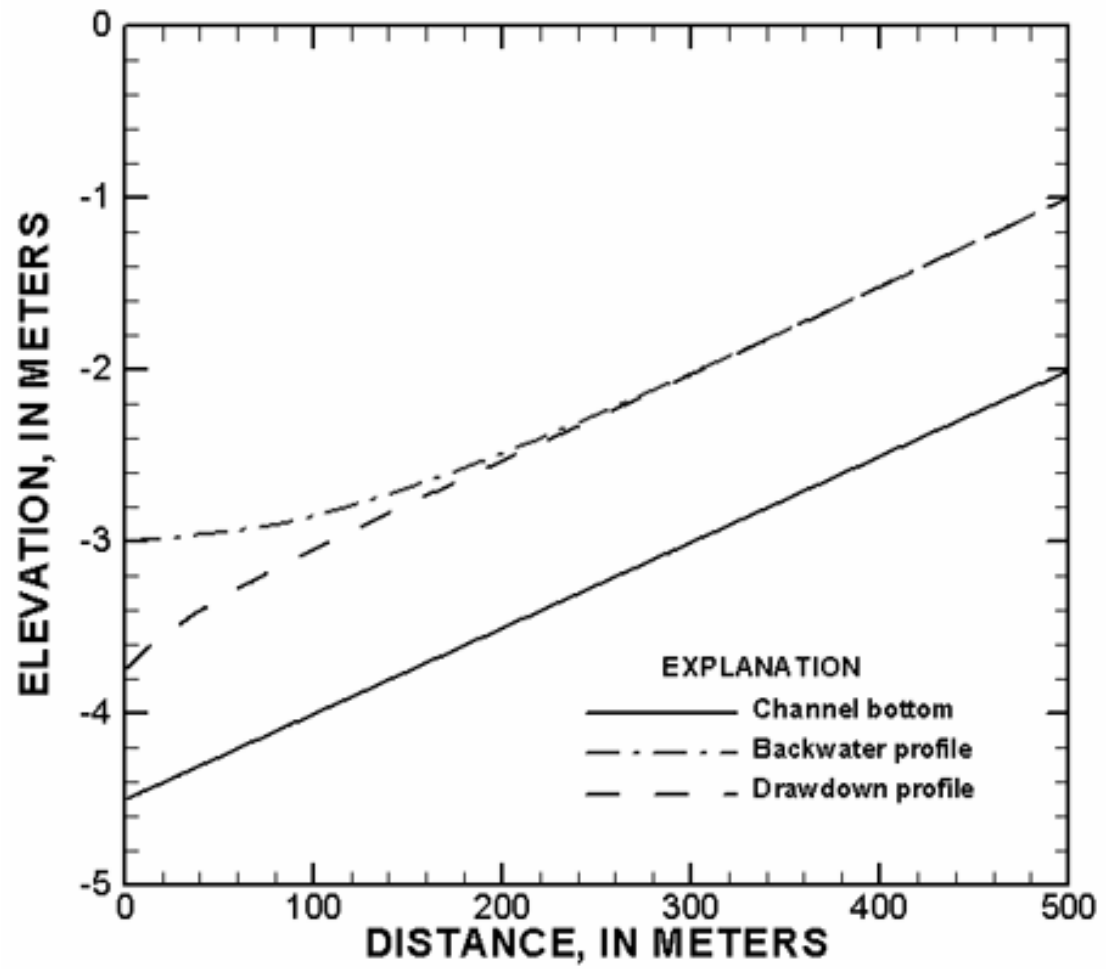

Figure 7. Simulated water-surface profiles for scenario B with a roughness of 0.075 and a uniform depth of 1 meter

The computed uniform depth for the two simulations is 1.06 m and is 6 percent larger than the 1.00-meter depth computed by the Manning's equation. The depth is in equilibrium at about 870 m and 865 m from the outflow end for the backwater and drawdown curves, respectively (fig. 8).

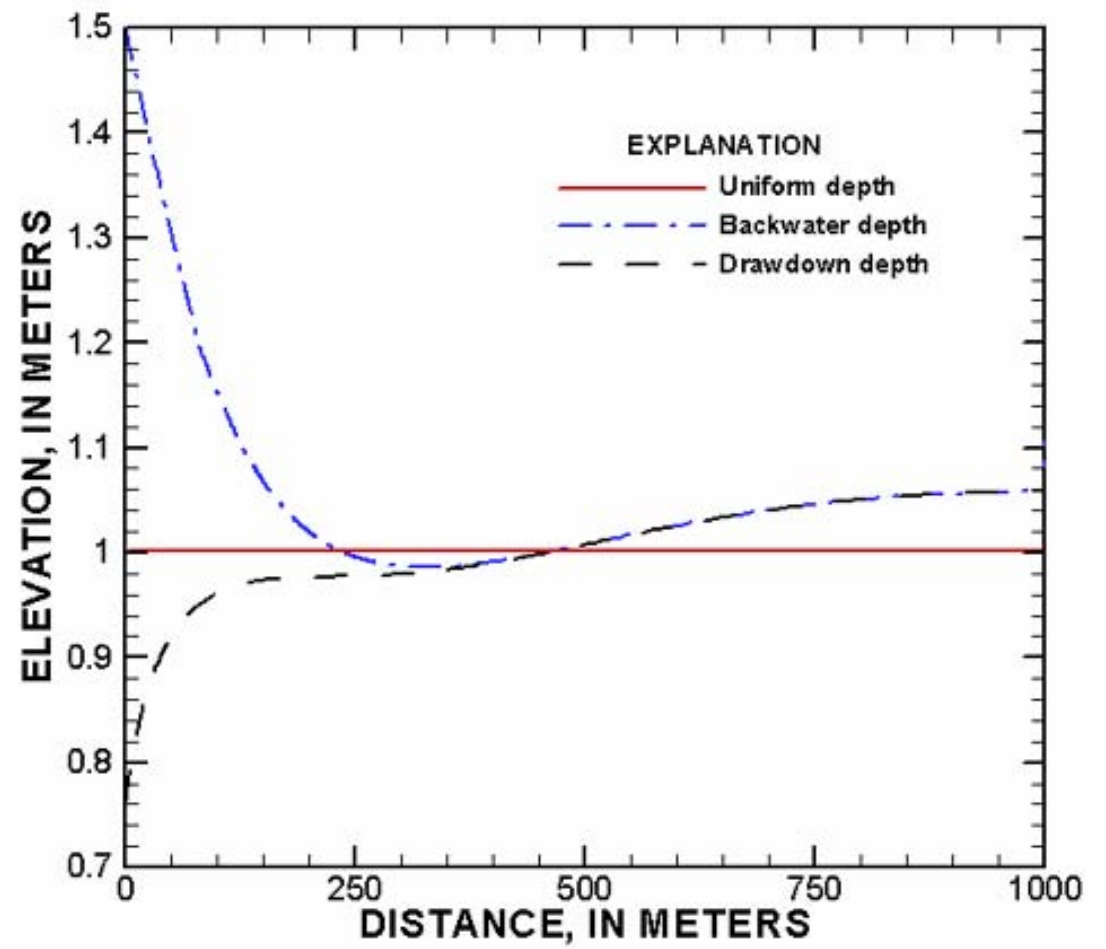

Figure 8. Simulated flow depth for scenario B with a roughness of 0.075 and a uniform depth of 1.0 meter

Davidian (1984), in addition to the previous equation, presents an empirical equation for estimating the distance needed for a downstream water depth that is 75 percent of uniform depth to converge to uniform depth for subcritical-flow conditions (M2 curve):

$$\frac{LS_o}{Y_n} = 0.57 - 0.79F^2 \quad . \qquad \textbf{(24)}$$

For a water depth of 0.75 m at the outflow boundary, the length of reach needed to approach within 3 percent of uniform depth is 100 m for equation (24), compared to 110 m for the simulation. However, the simulation does not converge to a flow depth that is within 3 percent of the uniform depth of 1.0 m. If the criterion is changed to be 3 percent of the depth to which the model converges, 1.06 m, the length of reach needed for convergence is about 594 m. The plot of flow depth with channel distance in figure 8 illustrates the convergence of the simulation to uniform depth. As in the previous simulation, the backwater curve undershoots the uniform depth before converging. For

the drawdown curve the simulation reaches a depth that is 98 percent of the uniform flow depth about 150 m from the outflow end. For distances greater than 450 m from the outflow end, the depth is greater than normal depth.

Scenario C: Roughness of 0.012 With Uniform Depth of 3 Meters

The third scenario is for a roughness of 0.012 that is typical for smooth concrete-lined channels. Supercritical flow occurs for each simulated profile. Water-surface profiles for outflow water depths of 6.0 m and -0.27 m are shown in figure 9 for equilibrium conditions. Because the flow for this scenario is more advective than the two previous scenarios, a 0.04-second time step is necessary. Steady conditions were reached for the outflow depth that was less than the uniform depth within 10,000 time steps. For the outflow depth that is subcritical and greater than uniform depth, a hydraulic jump (an abrupt jump in water surface) initially occurs in the channel. During the simulation, the jump migrated to the outflow end. For this case, more time steps were required for the jump in the water surface to travel out of the channel reach. Steady conditions were reached within 20,000 time steps.

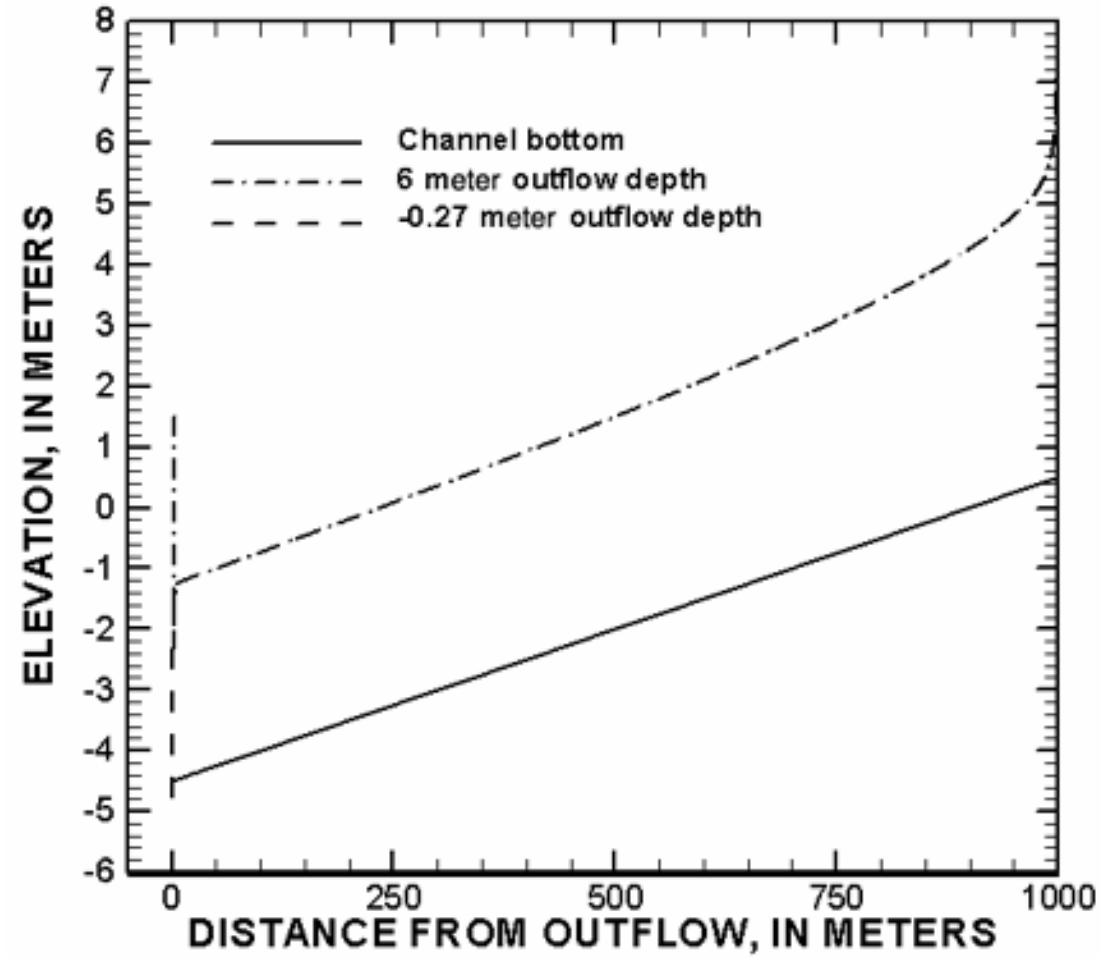

Figure 9. Simulated water-surface profiles for scenario C with a roughness of 0.012 and a uniform depth of 3 meters

The simulated depth near the outflow boundary is 3.25 m and is 8 percent larger than the value computed by the Manning's equation. Simulated depths are shown in figure 10. The computed depths near the outflow boundary may not be in equilibrium with gravity and friction. It is possible that a lower equilibrium flow depth near the outflow would be simulated if the channel were longer.

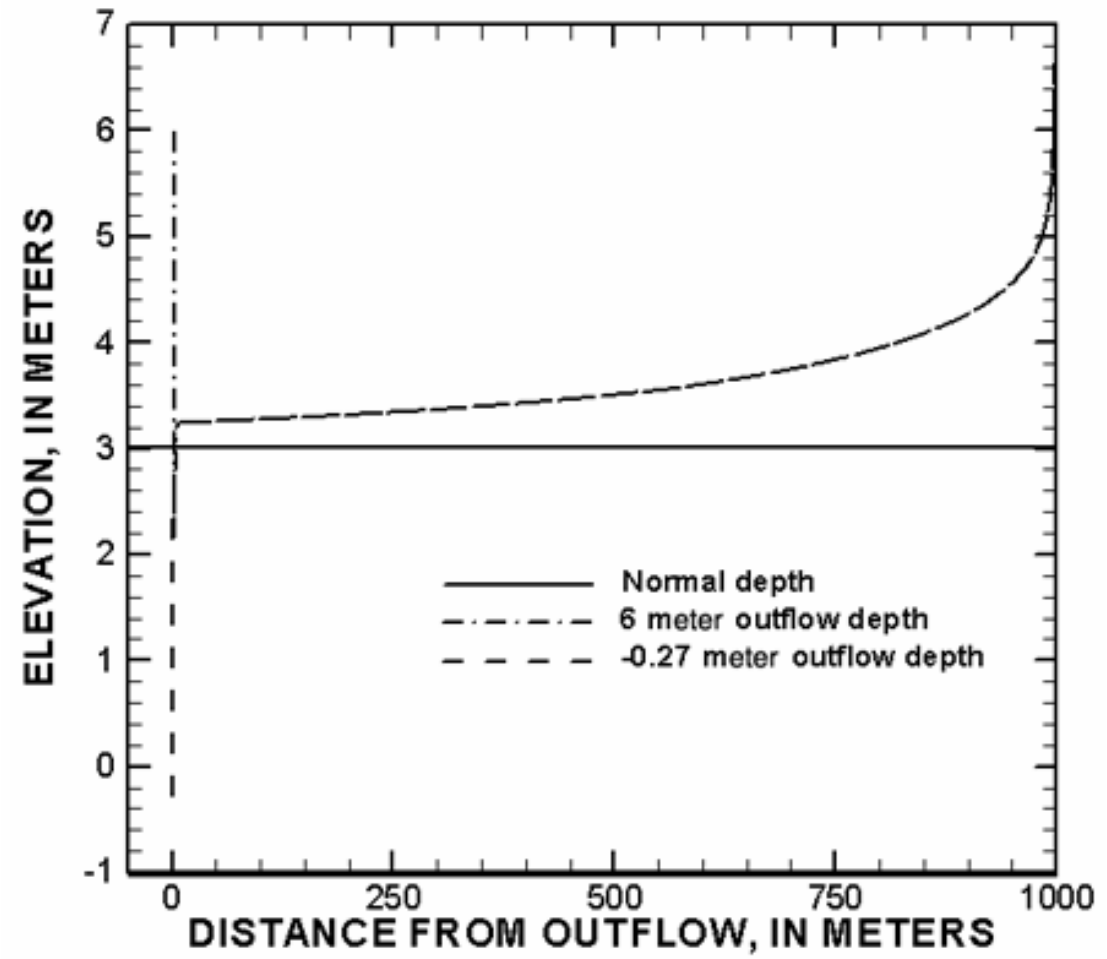

Figure 10. Simulated flow depth for scenario C with a roughness of 0.012 and a uniform depth of 3.0 meters

Possible Sources of Simulation Error

TrimR2D uses a constant flow depth within a cell. It is unlikely that this causes a significant error because the channel slope is constant. Error in the simulated normal depths did not decrease with increasing flow depth or correlate with roughness values. It may be that a higher mesh resolution could have reduced the error in simulated flow depth. Alternatively, the error in the simulated flow depths may be due to the numerical scheme used. No attempt was made to increase the model's mesh resolution because of time constraints.

Laboratory Dam-Break Simulation

Simulating a transient flow, such as a dam break, gives insight into how appropriately the advective terms are computed. Dam breaks typically generate steep, rapidly changing hydrographs that can challenge the computational stability of many numerical schemes. This section presents results from simulating a dam break.

The dam break simulated is one of many laboratory experiments (Schmidgall and Strange, 1961) conducted by the U.S. Army Corps of Engineers (COE) during the 1950s to obtain stage and discharge data from dam breaks. The experiments were performed in a 121.92-meter-long laboratory flume with a 1.219-meter-wide rectangular section and a slope of 0.005. The dam was located at the midpoint of the flume length. The experiments simulated the sudden failure of a dam retaining a pool of water.

The dam-break flow was for a constant inflow of 0.08767 m^3/s and an initial flow depth of 0.1707 m downstream of the dam. The base flow was passed beneath the dam. Roughness elements, consisting of 0.4445-centimeter (cm) aluminum angles, were installed on the flume floor perpendicular to the flow at 0.1524-m intervals. One leg of the aluminum angle was tacked to the flume floor, resulting in a roughness element height of 1.905 cm. Manning's roughness coefficients estimated from uniform flow experiments were 0.04 at 0.21340-meter flow depth and 0.12 at 0.04572-meter flow depth. Total duration of the hydrograph following the dam failure was 240 seconds, with a peak discharge of 0.1500 m^3/s. Measured data are available for the experiment at several locations in the channel. Simulation results for two portions of the flume are presented: (1) a 38.1-meter reach downstream of the dam and (2) a reach that included both the impounded pool behind the dam and the reach downstream of the dam.

Reach downstream of dam

This simulation was for a portion of the laboratory flume downstream of the dam. The reach is located in the laboratory flume between 7.62 m and 45.72 m downstream of the dam. The computational mesh for the 38.1-meter-long reach has a square cell size of 0.3048 m. The mesh is 6 cells wide by 125 cells long. The exit elevation of the flume in the computational mesh is 0.0 m. As for the uniform depth simulations, cell topography elevations on three sides of the computational mesh prevented flow through the mesh sides for all flows.

The dam-break data for this reach are not very difficult to simulate accurately with typical one-dimensional, unsteady flow models. Fulford (1998) found that one-dimensional models using a four-point implicit numerical method matched the dam-break hydrograph well. In the study, the roughness coefficients were adjusted for "dead" water behind the aluminum angles but were not altered to improve the fit of the one-dimensional models to the data.

The measured data for downstream water-surface elevation and upstream source discharge were used as boundary conditions. Discharge was divided equally among the four center nodes at the head of the flume. A converged solution computed by the TrimR2D model for a constant flow of 0.08767 m^3/s and a depth of 0.1707 m was used as the initial conditions for the simulation. A time-step size of 0.1 second was used. The

roughness value was determined by adjusting the roughness value until the simulated flow depth approximately matched the flow depth measured for the initial discharge. The calibrated roughness was 0.055 and results in a 0.0035-meter underestimation of the flow depth at the inflow end of the reach downstream of the dam.

Timing of the initial rise of the simulated peak (fig. 11) is good when compared with data measured at a location 21.34 m upstream of the outflow boundary (or 36.58 m from flume end). Simulated water-surface elevations (fig. 11) are generally lower than the measured values. During the recession of the peak, between 75 and 180 elapsed seconds, the simulated elevations match the measured elevations well. Simulated water-surface profiles at 1, 15, 30, and 55 elapsed seconds are plotted in figure 12. The plots of simulated water-surface profiles show that the rise in the water-surface elevation at 21.34 m upstream of the outflow boundary is due mainly to the change in the downstream water elevation.

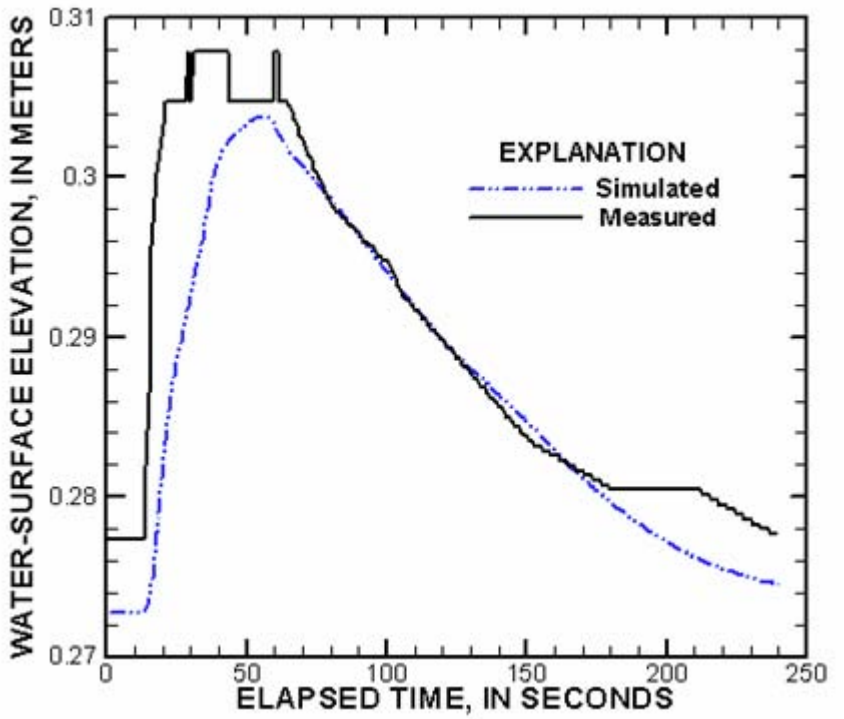

Figure 11. Hydrographs for site located 21.335 meters upstream of the outflow boundary

Modeled reach is downstream of dam

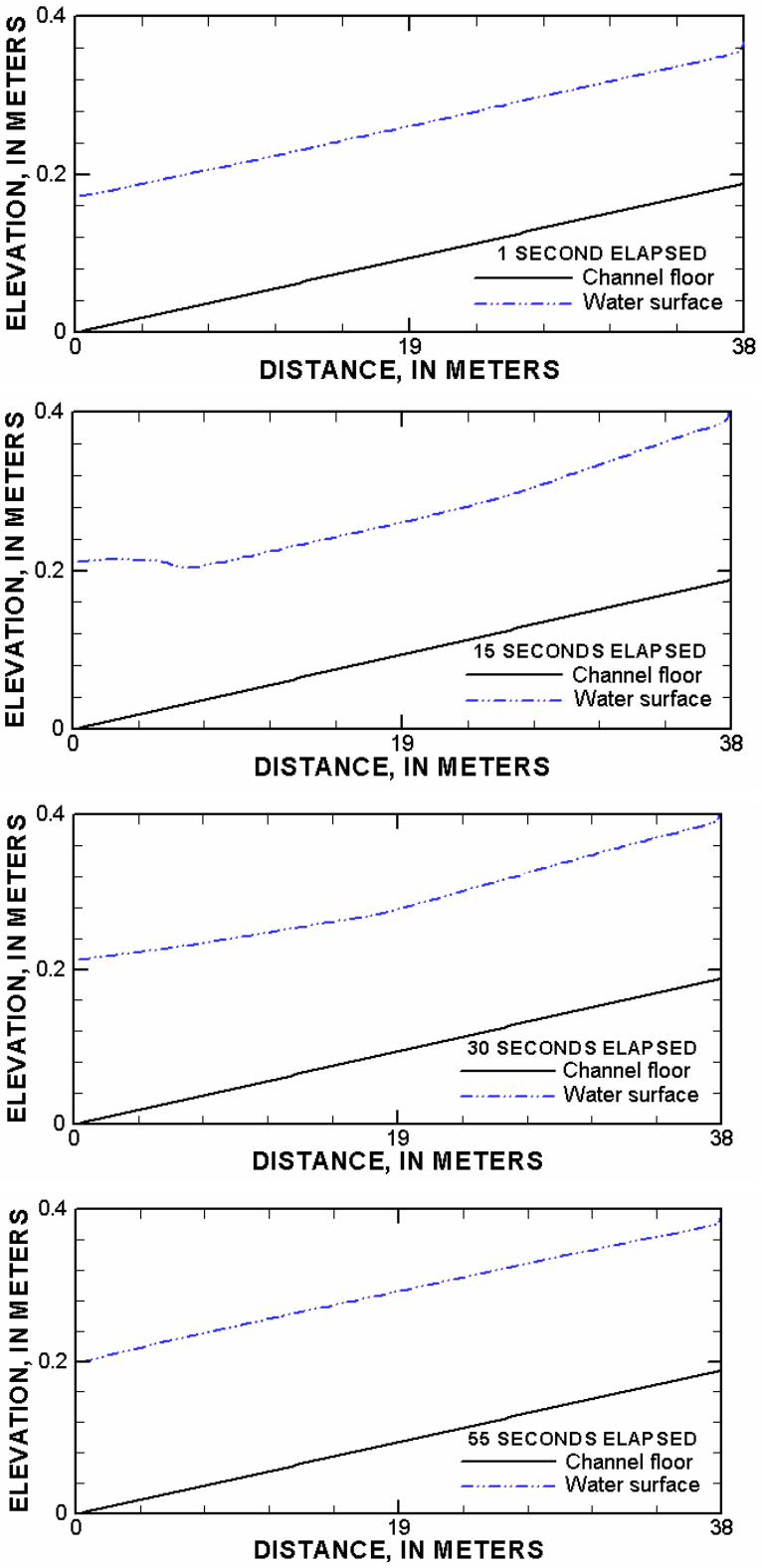

Figure 12. Simulated water-surface profiles of reach downstream of dam at 1, 15, 30, and 55 seconds elapsed from start of simulation

Some of the error in the simulation may result from the use of point sources to inject the discharge into the model. Sources add flow volume to the model in the continuity equation and do not directly affect any of the terms in the momentum equations. Thus, any momentum (or the effects of velocity) from incoming flows is neglected by TrimR2D. The abrupt front of the wave from the dam break is likely smoothed by the omission of the momentum forces associated with the inflow velocity. The omission of inflow momentum effects may be causing the simulated peak to arrive later than the measured peak at the measurement site located 21.335 m upstream of the outflow boundary (fig. 11). Much of the fit in the hydrograph (fig. 11) at this location is the result of the propagation of the water-surface elevation boundary condition upstream from the outflow end.

Pool behind dam and reach downstream of dam

This simulation is for the portion of the laboratory flume that includes the impounded pool upstream of the dam and the reach downstream of the dam. This reach is especially challenging because of the abrupt change in water-surface elevation located at the face of the dam that occurs when the dam is removed. Many flow models, such as RMA2 (U.S. Army Corps of Engineers, 1996), Branch (Schaffranek and others, 1981), and FESWMS (Froehlich, 1989), are unable to compute for discontinuous or nearly discontinuous water-surface elevations or for changes in flow regimes. Typically, flow models will have computational errors that will prevent the model from running over the specified period.

Initially, the simulation was made for the portion of the flume beginning 49.28 m above the dam and ending 45.72 m below the dam. The initial-condition file used was a composite of two restart files computed with TrimR2D: a file with an outflow depth of 0.1707 m and a file with an outflow depth that created an appropriate water-surface profile upstream of the dam. The resulting initial-conditon file represented the abrupt jump in water-surface elevation at the dam face. Boundary conditions were a constant inflow of 0.08767 m^3/s and a time-varying stage measured in the laboratory at a location 15.24 m from the flume outflow end. A solution was computed for all time steps. However, results from this simulation did not match measured values.

The simulation therefore was repeated for the entire 121.92-meter flume length. The computational mesh used for the flume is a 6-by-410-cell mesh composed of 0.3048 m-square cells. A small change in elevation at the end of the flume was included in the topographic mesh to represent the height of an angle iron. Because the flow free falls out of the flume end in this simulation, it is likely that the flume edge condition affected the height of the backwater curve. The simulated flume has a roughness of 0.05. The selected roughness value was determined by matching the flow depth at a location 15.24 m upstream of the flume outflow end.

Initial conditions were created by placing a weir at the location of the dam in the topographic mesh and by letting the simulation reach steady conditions. The weir height was determined by adjusting the height until the pool depths approximately matched measured values upstream of the dam. The constant inflow discharge of 0.08767 m^3/s was divided equally among the four center nodes at the head of the modeled reach, outside of the backwater zone produced by the dam.

The simulation of the dam break used the initial conditions with a topographic mesh that omitted the weir. Boundary conditions were the same as for the initial-condition simulation, constant inflow and free fall outflow. A time step of 0.02 second was used for the 240-second simulation.

The simulated and measured water-surface elevation hydrographs for a location 36.58 m upstream from the flume end are shown in figure 13. Timing of the initial rise of the simulated peak compares well with the measured data. The simulated water-surface elevations are biased higher than the measured values. This possibly is because the roughness calibration procedure focused only on the measured location at 15.24 m upstream of the flume end.

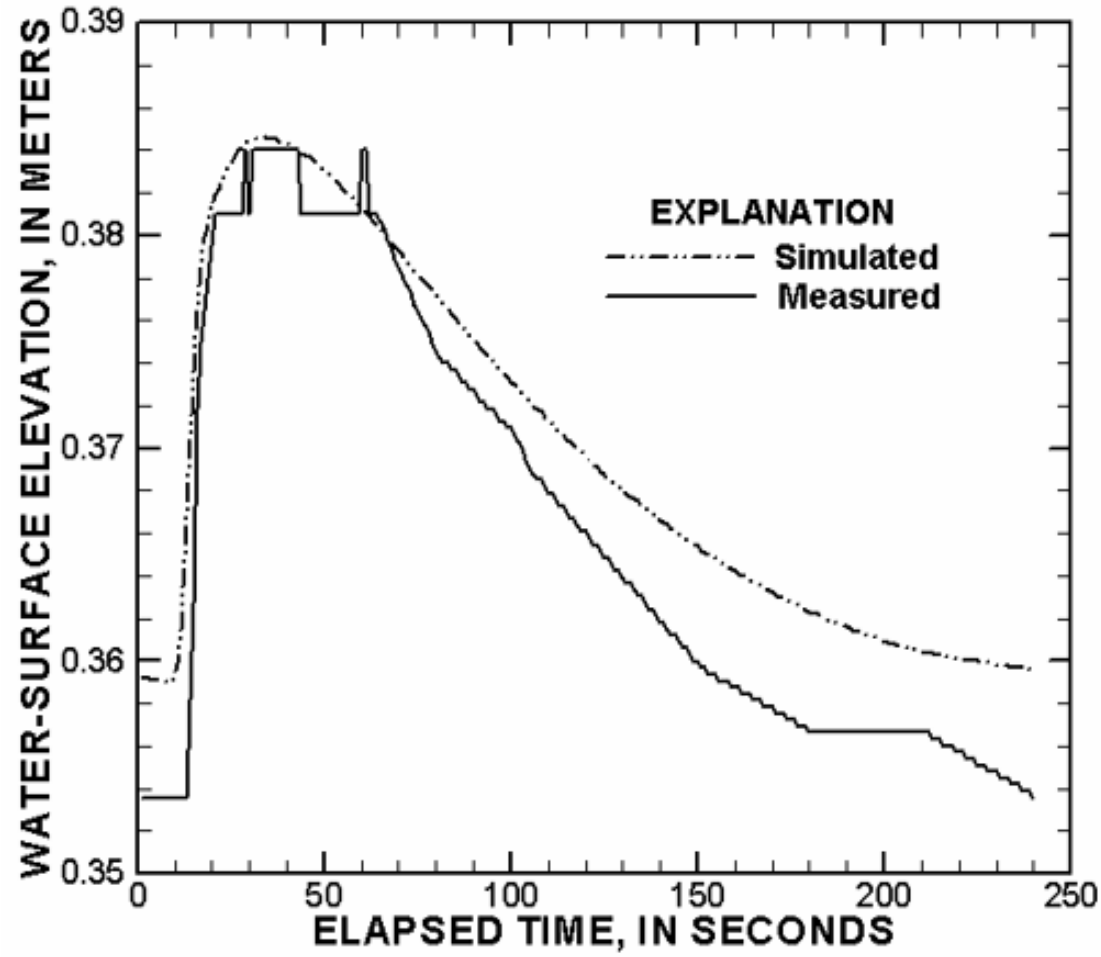

Figure 13. Hydrographs for site located 36.58 meters upstream of flume end

Modeled reach includes pool behind dam and reach downstream of dam

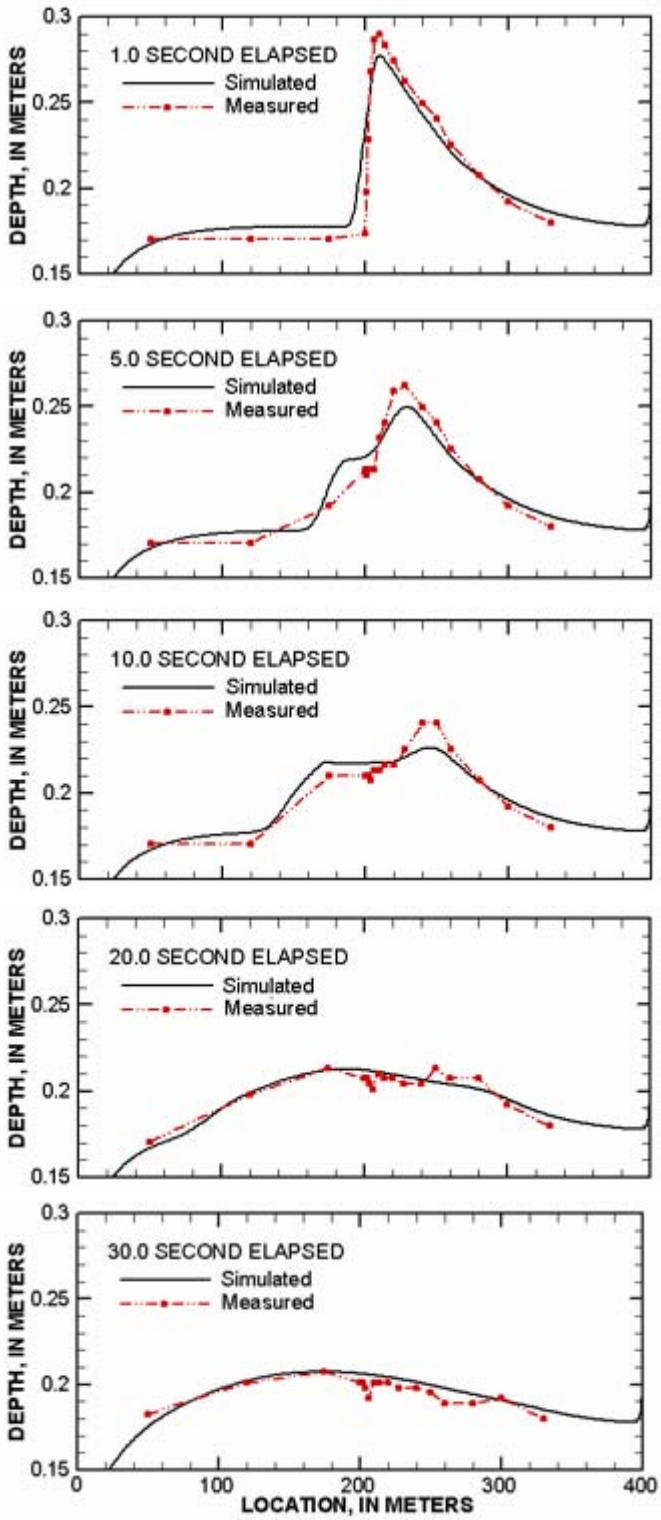

Figure 14. Measured and simulated water-depth profiles for pool behind dam and reach downstream of dam at various elapsed times. Dam is located 45.72 meters from outflow end

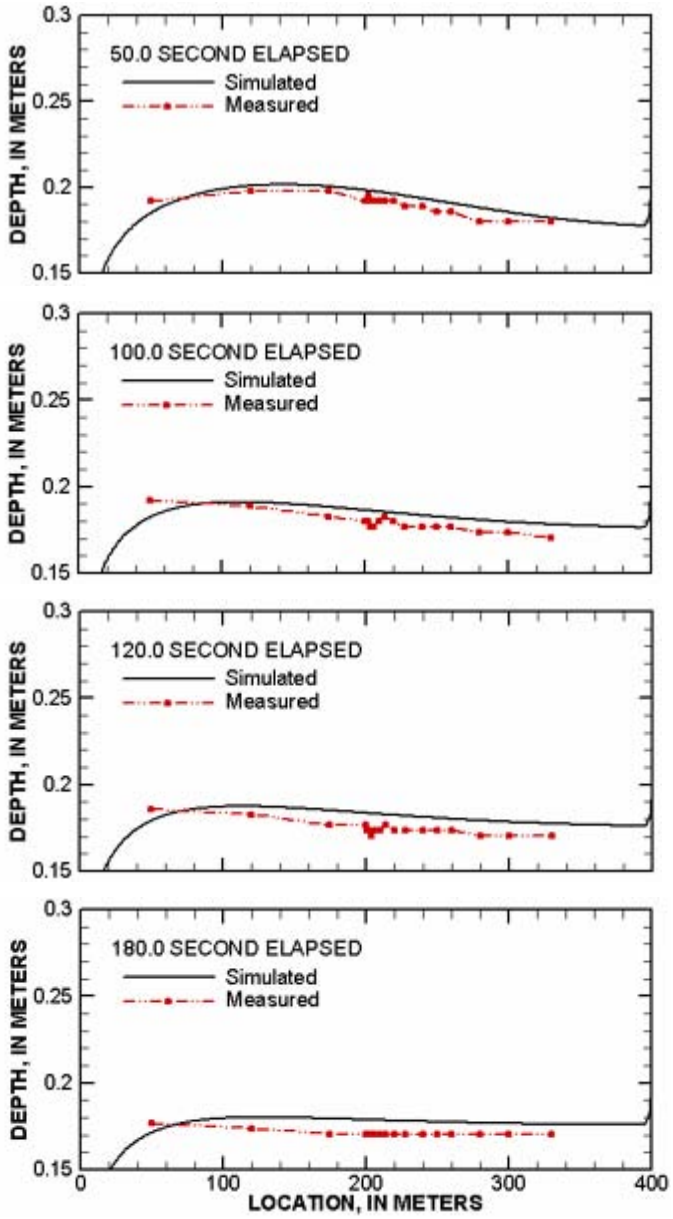

Figure 14. Measured and simulated water-depth profiles for pool behind dam and reach downstream of dam at various elapsed times. Dam is located 45.72 meters from outflow end—*Continued*

Simulated and measured flow depth profiles for the laboratory flume are shown in figure 14 for various simulation times. The computed depths match the measured depths very well for the simulation. Tables 2 and 3 present the percent errors between the simulated depths and the measured depths as a function of time and location, respectively. Generally, errors are less than +/-5 percent for the simulation. Based on location in the flume, average percent errors are largest near the dam location and smallest near the inflow end. Based on simulation time, average percent errors initially

declined to about 0.76 percent and then increased to about 4 percent over the duration of the simulation.

Table 2. Mean and standard deviation for percent error of simulated flow depths as a function of time

	Time (seconds)										
	0.5	**1.**	**5.**	**10**	**20**	**30**	**50**	**70**	**100**	**120**	**180**
Mean	1.44	2.71	0.76	0.76	0.90	2.06	2.27	2.99	3.01	4.23	3.90
Standard deviation	8.92	10.3	3.92	3.35	2.37	2.31	1.68	2.27	2.25	2.21	1.77

Table 3. Mean and standard deviation for percent error of simulated flow depths as a function of flume location

	Node location										
	50	**120**	**175**	**200 Dam**	**201**	**204**	**210**	**220**	**250**	**280**	**330**
Mean	-2.94	2.37	2.97	9.07	6.06	3.19	1.50	1.00	-0.17	1.82	3.32
Standard deviation	1.21	1.42	2.22	12.6	5.70	3.66	3.19	3.40	4.04	2.73	0.79

Large-Scale River Simulations

This section presents results for two large-scale river simulations—a reach in the Chattahoochee River, Georgia, and a reach in the Snoqualmie River, Washington. Both simulations demonstrate the accuracy of the TrimR2D model applied to large river reaches.

Chattahoochee River Simulation

The Chattahoochee River simulation is for a 15-kilometer reach of the Chattahoochee River in northeastern Georgia. Data used in the simulation were collected by the USGS (Faye and Cherry, 1980) for the period of March 22-23, 1976. The data include flow, water-surface elevation, and cross sections. Cross sections are available at approximately half-mile intervals along the length of the river. The datum for the cross-section elevations is the National Geodetic Vertical Datum of 1929. Cross-section locations are referenced to river distance. Cross sections are not referenced to a common horizontal (northing and easting) datum.

The simulated reach is from Littles Ferry Bridge, downstream of Buford Dam, to Georgia Highway 141. Flow data for the Chattahooche River at Littles Ferry Bridge and a tributary, Suwannee Creek, and stage data for Georgia Highway 141 were used as boundary conditions. Flow and stage data at Georgia Highway 120, located about 8.5 km downstream from Little Ferry Bridge, were used for comparison with the simulated values. Flow in the study reach is affected by the release of water that accompanies the

generation of hydroelectric power at Buford Dam. Flow released from the dam increased from 16.99 m^3/s on the morning of March 22 to 113.27 m^3/s. This flow was maintained for about 20 hours before returning to the low flow. Subsequently, a peak flow of 226.53 m^3/s, typical of a hydropower dam operations, was released on March 23.

The topographic mesh was interpolated from 19 cross sections using a square cell size of 4.8768 m. The cross sections were not referenced to a common horizontal datum in the report by Faye and Cherry (1980). This resulted in the mesh being a straightened-out representation of the actual reach and is similar to that used by one-dimensional flow models. Maps of the area could have been used to adjust the cross-section locations in the horizontal plane. However, it was not done because the horizontal adjustment would have required considerable effort and would have produced a large mesh of mainly non-active cells because the flow event was confined to the "low water" channel. The resulting computational mesh was 22 cells wide by 2,999 cells long. As in the previous simulations, flow out of the model domain occurred only at the downstream end.

Initial roughness values were estimated from those presented by Faye and Cherry. Because roughness values vary spatially in the reach and TrimR2D does not permit spatial variation of roughness values, averaged values were estimated from data for cross sections located at the site of discharge measurements. Roughness values were adjusted to 0.035 for all flow depths. Various time-step sizes were tried, but a 60-second time step was the largest value that worked for this application.

Initial conditions were computed using steady-state boundary conditions: 16.99 m^3/s inflow at Littles Ferry Bridge, 4.6723 m^3/s inflow at Suwannee Creek, and a downstream water-surface elevation of 268.34 m. The initial water-surface profile computed from the steady-state boundary conditions for the modeled reach is shown in figure 15. The water-surface elevation simulated at the Georgia highway 120 crossing was 0.234 m higher than the measured value.

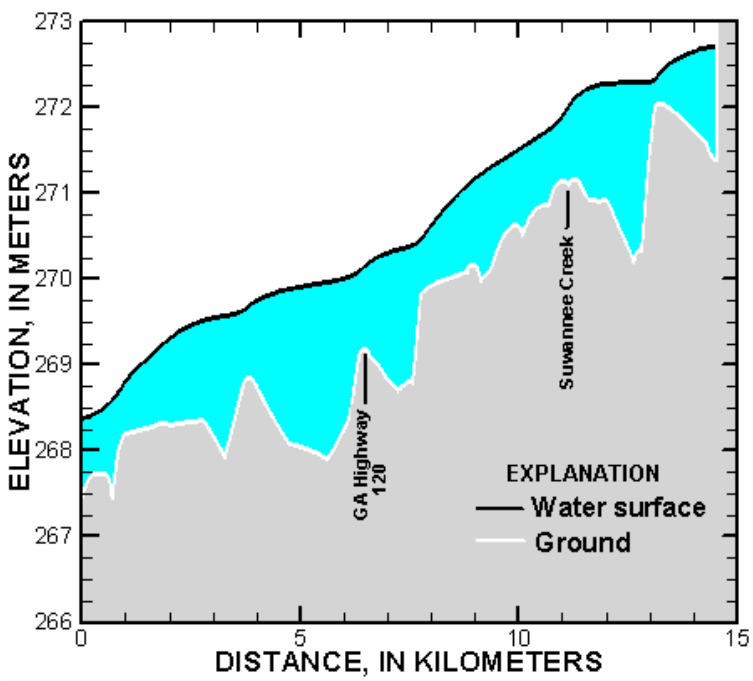

Figure 15. Simulated water-surface profile for initial conditions for the modeled reach of the Chattahoochee River

The arrival of the simulated peaks at the Georgia Highway 120 crossing matches the measured peak arrival well (fig. 16). The simulated water-surface elevation hydrograph for a 2-second time step matches the measured values well on the rises of the hydrograph. The computed hydrograph for a 60-second time step matches the measured hydrograph reasonably well. This hydrograph overestimates the peaks by approximately 0.05 m for the first peak and 0.1 m for the second peak. For both time-step sizes, the hydrographs for simulated water-surface elevations do not match as well on the recession of the peaks or at the lowest water-surface elevations. The simulated values for the lowest water-surface elevations were approximately 0.15 m larger than the measured values for both time-step sizes.

It is possible that the relatively poorer match at the lower flow depths is due in part to how the topographic mesh was constructed. Errors in mean flow lengths for water parcels between ground features in adjacent cross sections are expected to be largest for the lower flow depths and least for the higher flow depths. In spite of this gross approximation of the channel topography, the model fit very well the timing and magnitude of the measured flow peaks.

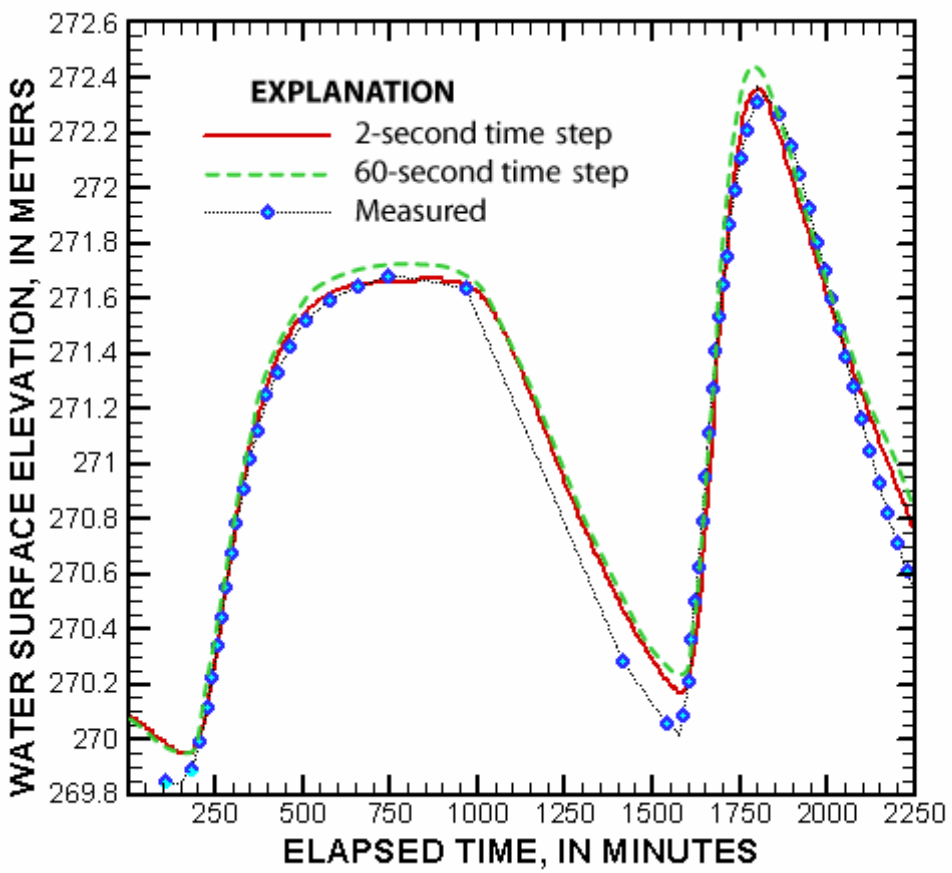

Figure 16. Hydrographs for March 22-23, 1976, at Georgia Highway 120 for measured and computed water-surface elevations for 2- and 60-second time-step sizes

Figure 17 shows the simulated water-surface profile for a 2-second time step at 1, 500, 1,000, 1,500, 1,750, and 2,200 elapsed minutes. The error caused by ignoring the momentum of the incoming flow is not evident in the water-surface profiles because the reach is much longer than the flume simulations. The proportion of the inflow momentum to the total momentum of the system is very small for this simulation.

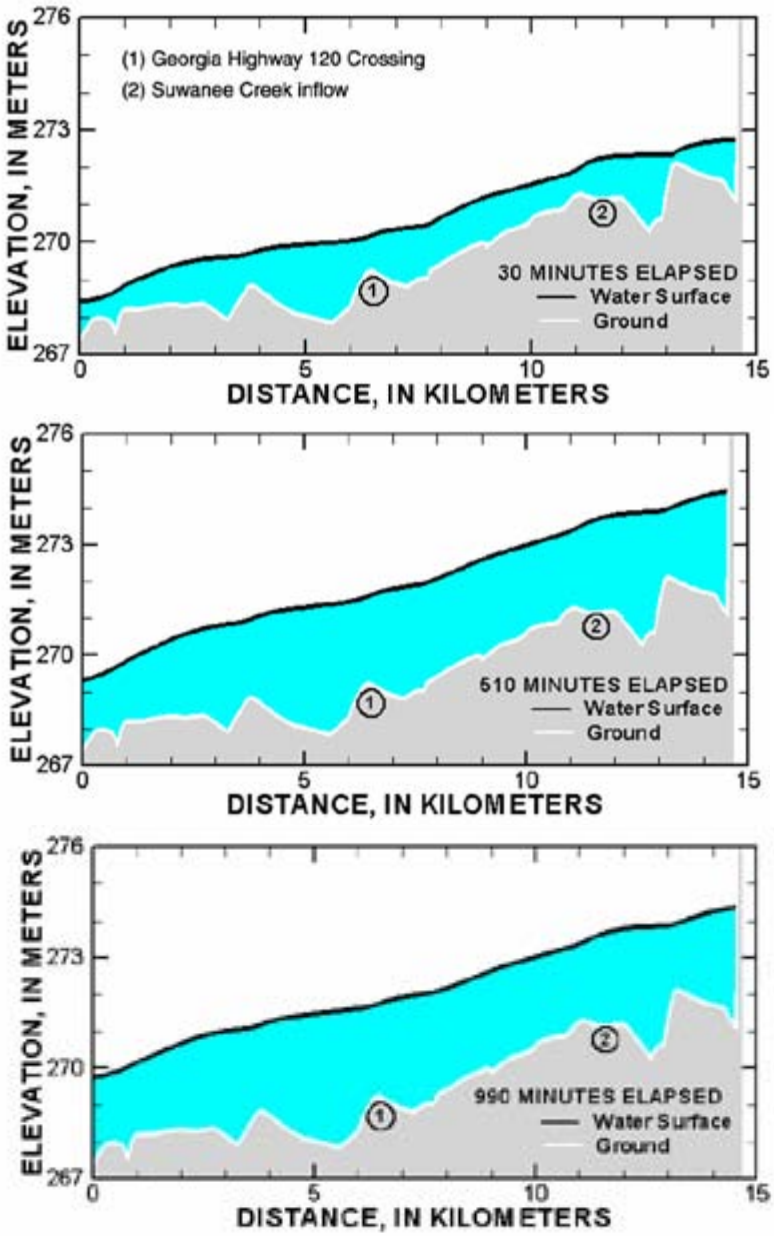

Figure 17. Simulated water-surface profiles of Chattahoochee River at 30, 510, 990, 1,500, 1,740, and 2,190 minutes on March 22-23, 1976

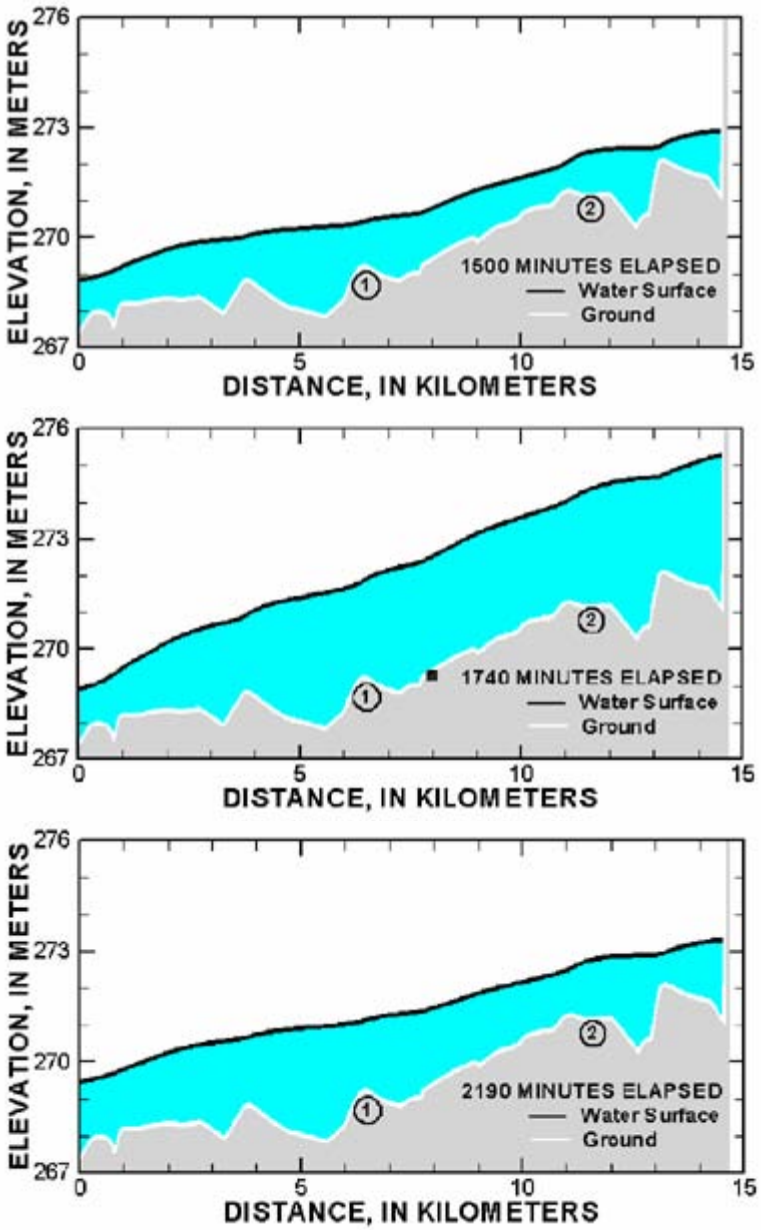

Figure 17. Simulated water-surface profiles of Chattahoochee River at 30, 510, 990, 1,500, 1,740, and 2,190 minutes on March 22-23, 1976—*Continued*

Snoqualmie River Simulation

The Snoqualmie River simulation is for a reach of the Snoqualmie River that is between Snoqualmie Falls and the Carnation Farm Road crossing of the Snoqualmie River. The simulated reach is about 27 km long and includes portions of the Raging and Tolt Rivers. The simulated reach covers an area that is 13,200 m by 8,240 m. The base 8-meter-resolution topography grid used is derived from 2-meter-resolution Lidar elevation data. The resulting model mesh is a 515-by-825-node mesh with a 16-meter resolution. Flow is not simulated for nodes that are located above a topography elevation of 45 m.

The Snoqualmie simulations use discharges measured at USGS streamflow-gaging stations Raging River near Fall City (12145500), Tolt River near Carnation (12148500), and Snoqualmie River near Snoqualmie (12144500) and the measured water-surface elevation at Snoqualmie River near Carnation (12149000) as the boundary conditions. Time-step size used for the simulations is 1.5 seconds. This time-step size allowed the model to propagate the flow across dry areas and maintain model stability for the flow events tested. Snoqualmie River simulations ran at about one half real time for the 1.5-second time step.

Two flow events were used to calibrate and verify the model, the flood events of November 24, 1986, and of December 3, 1975. Hourly inflow discharges for the calibration were computed from USGS stage hydrographs and stage-discharge ratings curves at the stream-gaging stations Snoqualmie near Snoqualmie (12144500), Raging River near Fall City (12145500), and Tolt River near Carnation (12148500). Measured data were not available for comparing the computed flooded areas with actual flood areas.

The 1986 flood event was used to determine (or calibrate) a Manning's roughness for the modeled reach. The event had a single peak (fig. 18). The calibration simulation period is from when the flow was contained to the low-water channel at the most upstream stream gage 12144500 (November 23, 1986, 1:00 a.m.) until the peak stage occurred at the most downstream gage 12149000 (November 24, 1986, noon). The measured peak discharge was 1,645 m^3/s at the most downstream gage, 12149000, and 1,617 m^3/s at the most upstream gage, 12144500. During the 1986 event, the Tolt River peaked before the flows at the most upstream and downstream gages 12144500 or 12149000.

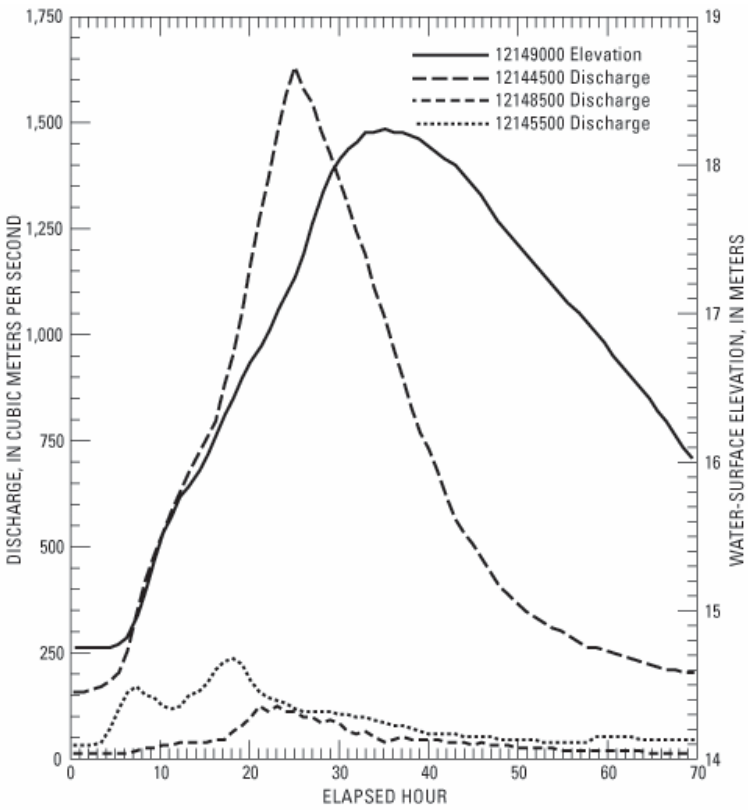

Figure 18. Hydrographs for the November 24, 1986, flood event for Snoqualmie River stream-gaging stations

Hydrographs begin on November 23, 1986, 1:00 a.m. and end on November 25, 1986, 11:00 p.m. (U.S. Geological Survey streamflow-gaging stations 12149000-Snoqualmie River near Carnation, 12144500-Snoqualmie River near Snoqualmie, 12148500-Tolt River near Carnation, and 12145500-Raging River near Fall)

The inflow discharge hydrograph for the Tolt River includes only the flow for the South Fork of the river. Flow for the North Fork of the Tolt was not available for the simulation. Because the flow contributed by the North Fork is small relative to the total Snoqualmie River flow, this error was not considered significant.

During calibration, the roughness value was adjusted until a reasonable match was obtained between the measured and simulated peak water-surface elevations. Manning's roughness values were varied from 0.035 to 0.120. Roughness values are constant in the Snoqualmie application regardless of flow depth. Simulated peak water-surface elevations for the 36-hour calibration hydrograph are shown in figure 19. Peak water-surface elevations were determined by selecting from the hourly model output the maximum elevation determined at each node over the simulation. Peak water-surface elevations were compared with peak elevations measured by the COE (U.S. Army Corps of Engineers, written commun., January 9, 2001) for the flood at five profile points located in the application reach (fig. 19). The accuracy of the peak water-surface

elevations measured by the COE is unknown. The best fit was for a Manning's roughness value of 0.12. Table 4 lists the measured and calibrated water-surface elevations for the five profile points. Errors for the calibrated peak water-surface elevations vary from -0.53m to +0.67m. Peak water-surface elevations are overestimated at the upstream profile points and are underestimated at the downstream profile points. The average error for the COE profile points is -0.11m and the average absolute error is 0.41m.

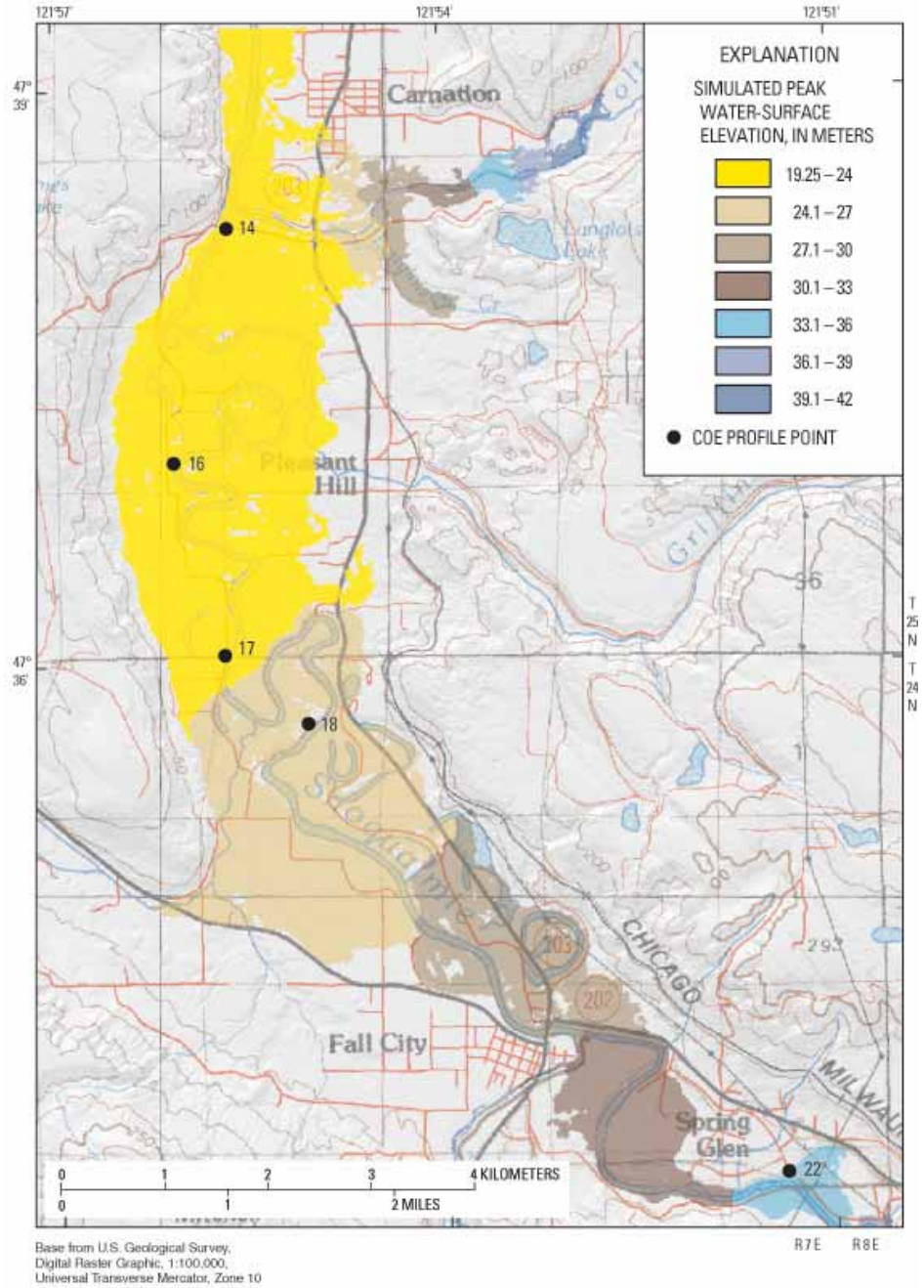

Figure 19. Simulated peak water-surface elevations on the Snoqualmie River for the November 24, 1986, flood event for a Manning's roughness value of 0.12

Peak elevations were measured by the U.S. Army Corps of Engineers at the five profile points

Table 4. Comparison of measured and simulated peak water-surface elevations for calibration of the Snoqualmie River model, using the flood event of November 24, 1986, and a Manning's roughness value of 0.12

COE profile point number (See fig. 19 for location)	Peak water-surface elevation (meters)		Error (meters)
	Measured	Simulated	
14	23.04	22.51	-0.53
16	23.77	23.04	-0.73
17	24.07	24.03	-0.04
18	25.35	25.29	-0.06
22	33.95	34.62	+0.67

The 1975 flood event was used for verification. The verification simulation period is from December 1, 1975, at 1:00 a.m. (while the flow was still confined by the low-water channel) and until December 3, 1986, at 11:00 a.m. (when the peak arrived at the most downstream gaging station 12149000). The flood event has multiple peaks at the most downstream gage, 12144500 (fig. 20). The peak discharge was 1,475 m^3/s at the most downstream gage and was 1,467 m^3/s at the most upstream gage, 12144500. Peak flow at gage 12149000 for the 1975 flood event was sustained for a much longer period than for the 1986 flood event used for the calibration. The flow at the Tolt initially peaked at about the same time as at the Snoqualmie gage.

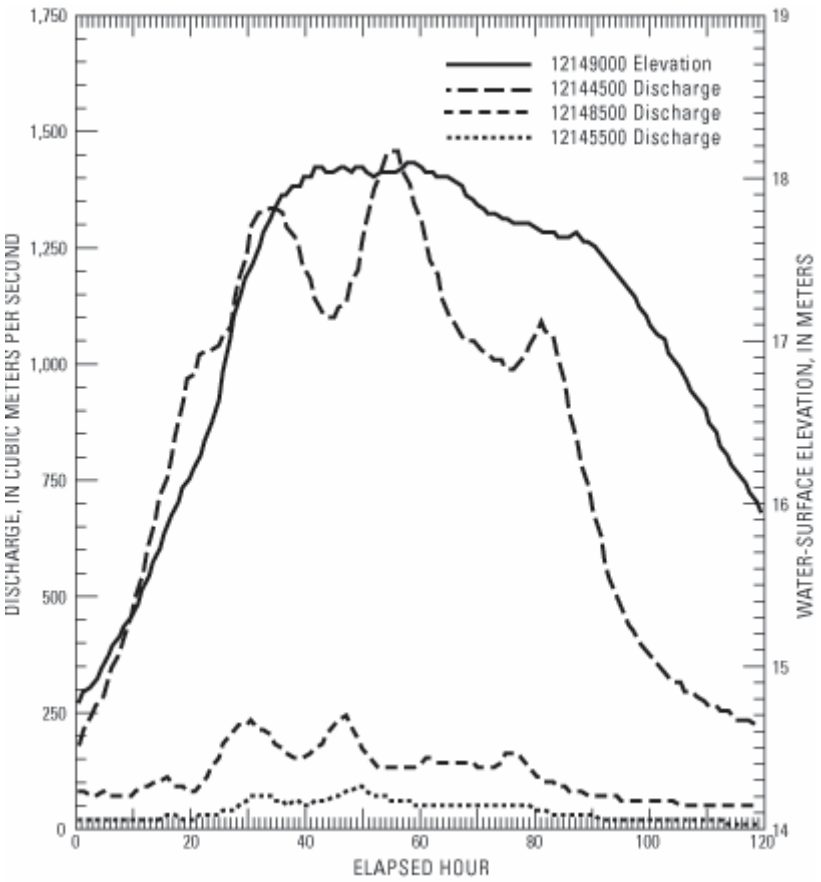

Figure 20. Hydrographs of the December 3, 1975, flood event for Snoqualmie River stream-gaging stations

Hydrographs start on December 1, 1975 1:00 a.m. and end on December 6, 1:00 a.m. (U.S. Geological Survey streamflow-gaging stations 12149000-Snoqualmie River near Carnation, 12144500-Snoqualmie River near Snoqualmie, 12148500-Tolt River near Carnation, and 12145500-Raging River near Fall City.)

Simulated peak water-surface elevations for the 59-hour verification hydrograph are shown in figure 21. Peak water-surface elevations were compared with those measured by the COE for the flood at five profile points located in the modeled reach. The accuracy of peak water-surface elevations measured by the COE is unknown. Table 5 lists the measured and simulated water-surface elevations for the five profile points for the verification event. Simulation errors range from -0.37 m to +0.68 m. The average error for the COE profile points is -0.09 m and the average absolute error is 0.36 m. Water-surface elevations are overestimated at the upstream profile point and are underestimated at the other profile points but are reasonable. The simulated water surface is flatter than the measured water surface. This may be because the mesh cell size or the time-step size is too large or because of errors in the measured peak water-surface elevations. No effort was made to decrease cell size or time step because of the excessively increased computational times needed for the available desktop computer system.

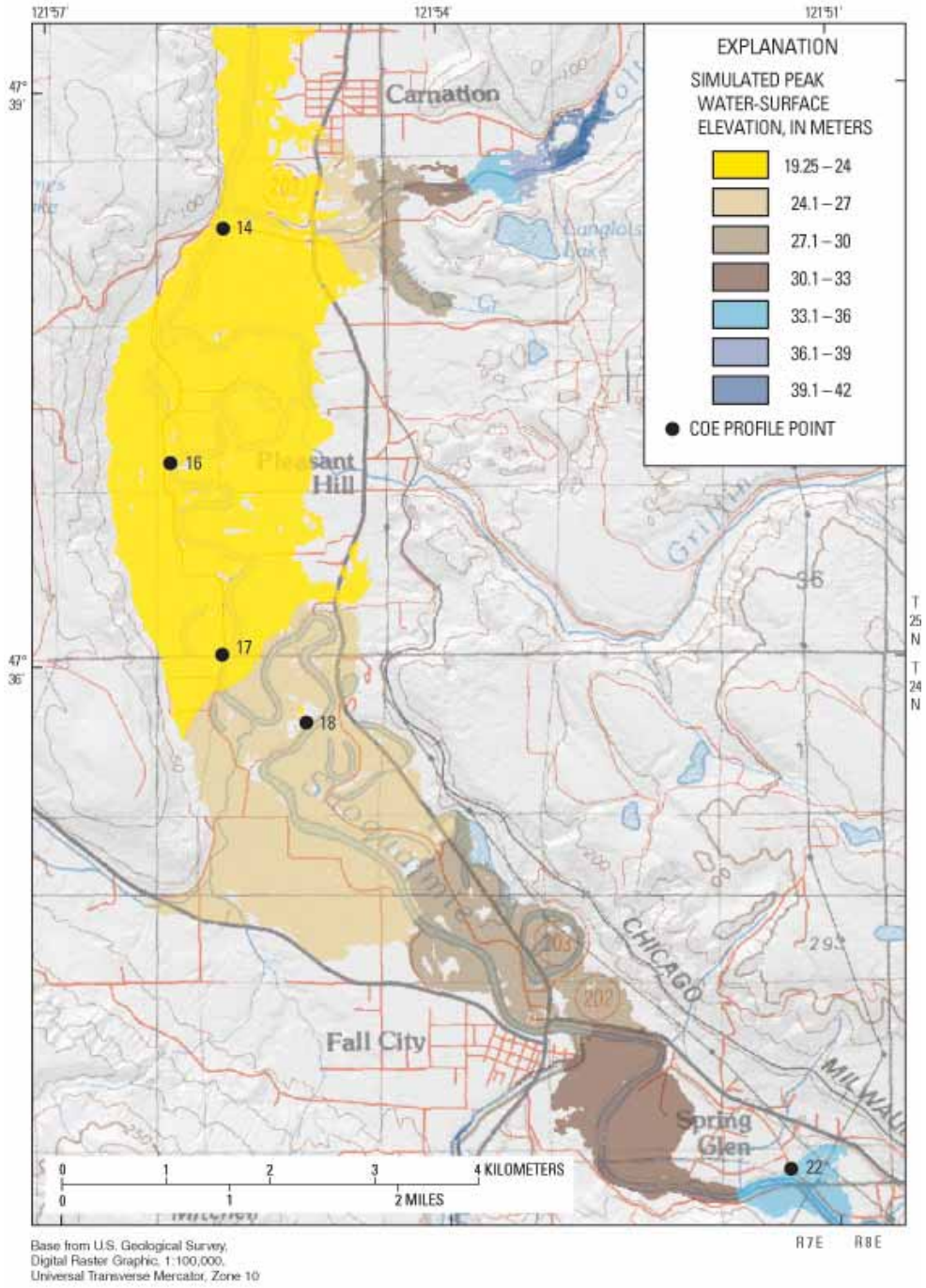

Figure 21. Simulated peak water-surface elevations on the Snoqualmie River for the December 3, 1975, flood event for a Manning's roughness value of 0.12

Peak elevations were measured by the U.S. Army Corps of Engineers at the five profile points

Table 5. Comparison of measured and simulated peak water-surface elevations for verification of the Snoqualmie River model, using the flood event of December 3, 1975, and a Manning's roughness value of 0.12

COE profile point number (See fig. 21 for location)	Peak water-surface elevation (meters)		Error (meters)
	Measured	Simulated	
14	22.94	22.73	-0.22
16	23.46	23.09	-0.37
17	24.22	24.01	-0.21
18	25.60	25.26	-0.34
22	33.80	34.48	+0.68

SUMMARY AND CONCLUSIONS

The numerical computer flow model Transient Inundation Model for Rivers – 2 Dimensional (TrimR2D) can be used successfully to model realistic river systems, as demonstrated by the Chattahoochee and Snoqualmie River simulations. It can model these systems accurately with less user intervention than some other two-dimensional depth-averaged flow models because it can simulate changes in flow regimes and cell wetting and drying. TrimR2D is best used in reaches where roughness does not significantly vary areally. For river systems, the solution should not be used near the inflow boundary, and the inflow boundary should be located several channel widths upstream of the area of interest because of the omission of inflow momentum.

Roughness values used in the uniform flow simulations do not precisely duplicate the results expected from Manning's equation. The model tends to over estimate uniform-flow depths. This behavior makes calibration of the roughness values used in an application important. Failure to calibrate the roughness values to measured data may result in over estimation of the water-surface elevations in the model.

Roughness parameters cannot be varied horizontally in the model. This limits model application to locations where areal roughness changes are not significant. Changes in areal roughness can dramatically affect flow patterns and water elevations. Flood plains where land use varies from agriculture to heavy woodland are an example where flood patterns are significantly affected by roughness changes. TrimR2D permits roughness values to change as a function of flow depth. In some situations, this may allow a higher roughness value to be used in the floodplain. In some situations, the current version of TrimR2D cannot accurately simulate flow where large changes in land use occur within the floodplain.

To simulate horizontal inflows appropriately requires the careful use of source terms. The inability to impart flows with momentum can result in errors for flows near the inflow boundary and in reaches of short length. For typical river systems, the error in the computations caused by ignoring the inflow momentum is minimized for stream

locations farther away from the inflow location. Alternately, inflow momentum can be imparted to the flow by using a pool (containing the source nodes) and weir at the inflow end of the mesh.

The Chattahoochee River data are typical for moderate-sized rivers. A good match of the hydrograph was found for the Chattahoochee River data at a location that was several kilometers downstream of the inflow location. This finding demonstrates that the model results can be used successfully when the locations of interest are sufficiently far from the inflow location. The Snoqualmie simulations demonstrated the ability of TrimR2D to propagate flow across a floodplain. Results for this simulation were reasonable.

TrimR2D is capable of handling large local changes in water surface and velocity without diverging from the solution. This feature permits the model to compute steady-state or initial conditions without user intervention and to run for cases that are not possible for models such as RMA2 and FESWMS. The normal flow cases demonstrated that the model can easily be started from a dry bed and converge to a solution, even with the presence of sharp water-surface gradients in the flow. This is in contrast to flow models such as RMA2 and FESWMS. Modeling and serving on the Internet of real-time flood inundation requires a model that will run with very little, if any, user intervention. TrimR2D requires less user intervention than other two-dimensional flow models. It is a robust model that is capable of giving accurate results for many types of river systems.

REFERENCES

Bates, P.D., and DeRoo, A.P.J., 2000, A simple raster-based model for flood inundation simulation: Journal of Hydrology, v. 236, p.54-77.

Casulli, V., 1990, Semi-implicit finite difference methods for the two-dimensional shallow water equations: Journal of Computational Physics, v. 86, p.56-74.

Casulli, V., and Cattani, E., 1994, Stability, accuracy and efficiency of a semi-implicit method for three-dimensional shallow water flow: Computers Math. Applications, v. 27, no. 4, p.99-112.

Cheng, R.T., Casulli, V., and Gartner, J.W., 1993, Tidal, residual, intertidal mudflat (TRIM) model and its applications to San Francisco Bay, California: Estuarine, Coastal and Shelf Science, v.36, p.235-280.

Chow, T.V., 1959, Open-channel hydraulics: New York, McGraw-Hill, p. 89-156.

Conte, S.D., and deBoor, C., 1980, Elementary numerical analysis: an algorithmic approach: New York, McGraw-Hill,
p. 356.

Davidian, J., 1984, Computation of water-surface profiles in open channels: Techniques of Water-Resources Investigations of the United States Geological Survey, Book 3, Chapter A15, p. 17-18.

Faye, R.E., and Cherry, R.N., 1980, Channel and dynamic flow characteristics of the Chattahoochee River, Buford Dam to Georgia Highway 141: U.S. Geological Survey Water-Supply Paper 2063, 65 p.

Fulford, J.M., 1998, Evaluation and comparison of four one-dimensional unsteady flow models: U.S. Geological Survey Water-Resources Investigations Report 98-4242, 33p.

Froehlich, D.C., 1989, Finite element surface-water modeling system: Two-dimensional flow in a horizontal plan - Users manual: Federal Highway Administration RD-88-177, 285 p.

Ostenaa, D.A., Levish, D.R., Klinger, R.E., and O'Connell, D.R.H., 1999, Phase 2 paleohydrologic and geomorphic studies for the assessment of flood risk for the Idaho National Engineering and Environmental Laboratory, Idaho: Bureau of Reclamation Report 99-7, 117 p.

Perry, C.A., March 2000, Significant floods in the United States during the 20th Century - USGS measures a century of floods: U.S. Geological Survey Fact Sheet 024-00, 4 p.

Schaffranek, R.W., Baltzer, R.A., and Goldberg, D.E., 1981, A model for simulations of flow in singular and interconnected channels: Techniques of Water-Resources Investigations of the United States Geological Survey, Book 7, Chapter C3, 110 p.

Schmidgall, T., and Strange, J.N., November 1961, Floods resulting from suddenly breached dams conditions of high resistance: Miscellaneous Paper No. 2-374, Report 2, U.S. Army Corps of Engineers Waterways Experiment Station, 117 p.

U.S. Army Corps of Engineers Waterways Experiment Station, 1996, Users guide to RMA2 version 4.3: U.S. Army Corps of Engineers, Waterways Experiment Station, Hydraulic Laboratory, 227 p.

Walters, R.A., and Denlinger, R.P., 1999, Appendix C- Description of flood simulation models: Bureau of Reclamation Report 99-7, 12 p.

Appendix A. File Specifications for Model Input and Output Files

The data needed for program execution and the results produced by the program are grouped into several files by type. The files containing data for program execution (input files) are designated by the file-name extensions .inp, .grd, .pts, and .win and the file name timebc.dat. They are free-format ASCII files and can be created with a text editor. Values must be separated by a space. Files containing program results (output files) are designated by the file-name extension .dat and tsdata.dat and the file name restart.dat. The restart.dat file is a binary file (unformatted) and can be used to supply initial conditions. The other files with .dat extension and the file tsdata.dat are column-justified ASCII files. The file contents and variable definitions of each file type are described in this appendix.

Program Control File

The program control file has a file-name extension of .inp and contains indices used in the numerical solution, filenames for files containing input data, roughness parameters, initial conditions, and output file parameters. The TrimR2D program queries the user with a file browser window for the name of this file when the program is executed.

File contents

Line number	Variables
1 - 2	comment lines describing simulation
3	comment line written to *.dat ASCII output file
4	FilenamesGRD
5	FilenamesPTS
6	FilenamesWIN
7	Outfilename
8	comment line containing names for parameters on following line
9	nskip, maxstp, nbegin, maxrex, nrstrt, noptype
10	comment line containing names for parameters on following line
11	epsi, qpsi, delt, theta, timebc
12	comment line containing names for parameters on following line
13	nlayer, wind-x, wind-y, zmin, etaobc
14	comment line containing names for parameters on following line
15	(n(k),k=1,nlayer+1)
16	comment line containing names for parameters on following line
17	(zn(k),k=1,nlayer+1)
18	comment line containing names for parameters on following line

19	nu-x, nu-y
20	comment line containing names for parameters on following line
21	ntsdata, ntsskip, tsscale
22	comment line containing names for parameters on following line
23	(irow(l),jcol(l),idf(l)), l=1,ntsdata

Variable definitions

FilenamesGRD – file name of grid file with .grd as the file extension

FilenamesPTS – file name of the discharge file with .pts as the file extension

FilenamesWIN – file name of the wind file with .win as the file extension

Outfilename – file name of the ASCII output file that contains program results

nskip – integer number of time steps to skip writing program results to the file Outfilename, starting at time step nbegin

maxstp – integer number of time steps executed in the simulation, elapsed time = maxstp x delt

nbegin – integer time step (as an integer) at which to start output of program results

maxrex – maximum integer number of iterations for the conjugant-gradient matrix solver

nrstrt - integer flag for the restart file read/write option. The restart file can be used as initial conditions for a simulation. Allowable flags are:

- 1 - an existing unformatted output file (restart.dat) is read and used as the initial conditions to initialize the dependent variables.
- 2 - an unformatted file (restart.dat) is written at the end of the computer run. The file contains the results for the last executed time step. This file can be used as an initial condition file.
- 3 - an existing unformatted file (restart.dat) is read and used as initial conditions and is written over with the results for the last executed time step.
- 5 - an existing unformatted file (restart.dat) is read and used as initial conditions. A free-format file, rstij.dat, that contains the i,j indices and the values for the dependent variables for the active nodes is written.
- 6 - the file rstij.dat is read and used to initialize the problem.

noptype – integer flag for output type:

- 1 – binary output files written at the requested time interval. The files have the name trimrout.nnn where nnn is the sequence number starting at 000.
- 2 – The ASCII output file with .dat extension where the output at each requested time interval is written in a separate zone. This provides a simple means for animation of the results in the commerical graphics program Tecplot™ by Amtec Engineering.

epsi – convergence tolerance for water-surface elevation, entered as a real number

qpsi – not used in two-dimensional model

delt – time-step size in seconds, entered as a real number

theta – time-weighting factor (values range from 0.5 to 1.0), entered as a real number. A typical value is 0.6.

timebc – integer flag for boundary-condition options:

- 0 - boundary conditions are time-independent (steady). The water-surface elevation in the boundary cells are set to the value etaobc and the discharge (or flow) values are given in the *.pts input file.
- $\neq 0$ – file timebc.dat is read for the boundary condition parameters.

nlayer – integer number of layers with separate roughness coefficients

wind-x – initial wind velocity in x coordinate direction (east-west), in m/s, entered as a real number

wind-y – initial wind velocity in y coordinate direction (north-south), in m/s, entered as a real number

dzmin – minimum flow depth or depth at which a node is considered dry, in meters, entered as a real number

etaobc – initial water-surface elevation, in meters, at the boundary cells (see fig. 4 in text), entered as a real number

n(k) – Manning's roughness coefficient for the kth layer, entered as a real number

zn(k) – the max depth, in meters, for which the Manning's roughness coefficient for the kth layer is applied, entered as a real number. The kth roughness coefficient is applied from the zn(k-1) to the zn(k) depths.

nu-x – horizontal eddy viscosity in the x-axis direction, in m^2/s, entered as a real number

nu-y – horizontal eddy viscosity in the y-axis direction, in m^2/s, entered as a real number

ntsdata – integer number of computational cells at which to write time series of simulation results

ntsskip – integer number of time steps to skip before writing simulation results for the selected cells to the time series file

tsscale – time scale for time-series output, entered as a real number. For instance, tsscale=60 gives a time scale in minutes.

irow(l) – x-axis (east-west) cell position (elevation node; see fig. 3 in text) of the lth time-series computational mesh location

jcol(l) – y-axis (north-south) cell position (elevation node; see fig. 3 in text) of the lth time-series computational mesh location

idf(l) – integer flag indicating the variable to output at the lth time-series location:

- 1 – water-surface elevation
- 2 - u component of velocity; $(u_{j-1/2} + u_{j+1/2})/2$

- 3 - v component of velocity; $(v_{i-1/2} + v_{i+1/2})/2$
- 4 - speed; $\sqrt{\left(\frac{v_{i-1/2} + v_{i+1/2}}{2}\right)^2 + \left(\frac{u_{j-1/2} + u_{j+1/2}}{2}\right)^2}$

Model Mesh (Grid) File

The model mesh (grid) file has a file-name extension of .grd and contains header data that describe the resolution (or cell dimension) and size (number of cells) of the regular rectangular mesh that is used by the model. It also contains the topography or ground elevations for the topography mesh. Ground elevations are specified for the user mesh at locations that are at half the spacing of the model grid. This eliminates the need to enter elevations for a staggered mesh. Elevations are referenced to a common vertical datum that is usually chosen to be the undisturbed water surface (or initial water-surface elevation) at the outlet. Elevations are positive in the downward direction and negative in the upward direction. The elevation values are read from upper left to lower right on a row-by-row basis.

File contents

Line number	Variables
1	nrow, ncol
2	dx, dy, x0, y0
3	hland, hsea, latitude, zscale
4 - last	(depth(i,j),i=1,nrow),j=1,ncol)

Variable definitions

nrow - integer number (or index) of user-supplied ground-elevation locations in the x-axis direction

ncol – integer number (or index) of user-supplied ground-elevation locations in the y-axis direction

dx – model mesh spacing, in meters, for the x-axis direction, entered as a real number. The value is the spacing between elevation locations in the user-supplied mesh or one-half the x-length of a mesh cell.

dy – model mesh spacing, in meters, for the y-axis direction, entered as a real number. The value is the spacing between elevation locations in the user-supplied mesh. The computational cells are square, so dy equals dx.

x0 – x-axis coordinate origin of the mesh, in meters, entered as a real number. This value is not used in the program.

y0 – y-axis coordinate origin of the mesh, in meters, entered as a real number. This value is not used in the program.

hland – elevation of permanently dry land, in meters, entered as a real number. Cells with elevations higher than hland are removed from the calculations. This value is compared to depth(i,j) x zscale.

hsea – elevation, in meters, used to detect water-surface-elevation boundary conditions within the mesh. This value is compared to depth(i,j) x zscale. Set to a value higher than hland and enter as a real number.

latitude – latitude, in degrees, used to compute the Coriolis force, entered as a real number. Because Coriolis forces are very small for riverine systems, set latitude = 0.

zscale – elevation scale, entered as a real number. All depth(i,j) are multiplied by this value. Use a value of –1.0 to convert elevation data to coordinate system used by model.

(depth(i,j),i=1,nrow),j=1,ncol) –ground elevation, in meters, listed starting at the upper left of the grid (1,1) and read row by row, ending at the lower right (nrow,ncol). Ground elevations are entered for all cells, including inactive cells.

Time-Dependent Boundary Condition File

The time-dependent boundary condition file, timebc.dat, is a free-format file. The file must be named timebc.dat and may be created using a text editor. TrimR2D can be compiled to use different or customized file-reading routines. Two versions of boundary file-reading routines are documented in this section. Both versions allow time-varying discharges to be specified for the cell locations identified in the intial-discharge file (file extension .pts). The first version (time_bc.for) is for locations where the boundary cells water-surface elevation can be represented by either a constant or harmonic function. The second version (timebc_interp.for) is for locations where a time series of water-surface elevations is used for the boundary cells water-surface elevation.

Harmonic Boundary Cell Water-Surface Elevation

This version can be used to set water-surface elevations in the boundary cells, $etaobc_h$, with the following equation:

$$etaobc_h = etaobc + \sum_{m=1}^{numhar} \left[amp(m) \sin\left(2\pi(freq(m)ts - phase(m))\right) \right]$$

File contents

Line number	Variables
1	numhar, numqbcs, numqsteps
2-(numhar*2 +1)	freq(m), amp(m), phase(m),m=1,numhar
(numhar*2 +2) – last	yr(ts), mon(ts), day(ts), min(ts),(ampq(s),s=1,numqbcs)

Variable definitions

numhar – number of harmonics in tidal water-surface-elevation boundary conditions

numqbcs – integer number of discharge-boundary locations, entered in the initial discharge file

numqsteps – number of discharges that are specified

freq(m) – frequency of tidal constituent, in cycles per second, for the mth harmonic, entered as a real number

amp(m) – amplitude of tidal constituent, in meters, for the mth harmonic, entered as a real number

phase – phase angle for tidal constituent, in degrees, for the mth harmonic, entered as a real number

yr(ts) – the year for the ts location in the time series, entered as an integer. The time series spans from the start to the end of the simulation.

mon(ts) – the month for the ts location in the time series, entered as an integer

day(ts) – the day for the ts location in the time series, entered as an integer

min(ts) - the minute for the ts location in the time series, entered as integer
(ampq(s),s=1,numbbcs) – the discharge values, in cubic meters per second, applied at time specified by yr(ts), mon(ts), day(ts), min(ts). The values are applied at the cell locations entered in the initial discharge file and are listed in the order specified in the initial discharge file.

Time-Series Boundary Cell Water-Surface Elevation

File contents

Line number	Variables
1	netas, nqnodes, cunits, zconstant, timestep
2-last	wsel(t), cellq(s),s=1,nqnodes

Variable definitions

netas – integer number of elevations. Always set to 1

nqnodes – integer number of inflow cells

cunits – multiplicative factor used to convert units in time-dependent boundary condition file to meters, entered as real number

zconstant – constant, in meters, to add to Wsel to shift elevations in the vertical, entered as a real number

timestep – time interval between entries in the file, in seconds, entered as a real number

wsel(ts) – outflow water-surface elevation at time ts, entered as a real number

(cellq(s),s=1,nqnodes) – discharge values, in cubic meters per second, at cell location s applied at time ts. The values are for the cell locations entered in the initial discharge file and are listed in the order specified in the initial discharge file.

Initial Discharge File

The initial-discharge file, with a file name extension of .pts, is read by free format and may be created with a text editor. The file specifies the cell locations at which discharge boundary conditions are supplied and the initial discharge value in m^3/s. The number of lines in the file is equal to the number of cells at which discharge boundary conditions are supplied, plus one.

File contents

Line number	Variables
1	names of parameters on following line
2 - last	ics, jcs, cellQ(ics,jcs)

Variable definitions

ics – east-west index in model coordinates of discharge node

jcs – north-south index in model coordinates of discharge node

cellQ(ics,jcs) – initial discharge, in cubic meters per second, for the ics, jcs cell

Wind-Data File

The wind-data file, with a file name extension of .win, is not usually used when river systems are simulated. It applies a wind velocity for a specified time over the entire computational grid.

File contents

Line number	Variables
1	Names for parameters on following line.
2 - last	hour, wx, wy

Variable definitions

hour – the elapsed hour at which to apply wind velocity. The elapsed hour is computed from the start of a simulation.

wx – wind velocity in the x-axis direction, in meters per second

wy – wind velocity in the y-axis direction, in meters per second

ASCII Output File

The ASCII output file, with a file name extension of .dat, is written when the variable noptype in the program control file (file extension .inp) is set to 2. The time is not written because a constant time interval is used for the file. Results are written at the time interval specified in the program control file (file extension .inp) by nskip. The output file name is entered in the program control file. The output file name must include the .dat extension. The file contains the results of the simulation in a format that can be

easily imported to a commerical graphics program, Tecplot™ by Amtec Engineering. All values are reported at the computational cell centers in order to simplify visualization.

File contents

Line number	Variables
1	Title information listed on line 3 of the *.inp file
1	ZONE I = inum,J= jnum
2 - last	i,j, h(i,j), eta(i,j,t), u(i,j,t), v(i,j,t), H(i,j,t)

Variable definitions

inum – number of cells in x-axis direction of grid

jnum – number of cells in y-axis direction of grid

i – x-axis cell location (or index)

j – y-axis cell location (or index)

h(i,j) – averaged ground elevation, in meters, referenced to the vertical datum at cell i, j

eta(i,j,t) – water-surface elevation, in meters, referenced to the vertical datum at cell i,j for time step t

u(i,j,t)- averaged x-axis velocity at cell i,j for time step t

v(i,j,t) – averaged y-axis velocity at cell i,j for time step t

H(i,j,t) – water depth in meters at cell i,j for time step t

Binary Output Files

Multiple binary output files are written when the variable noptype in the program control file (file extension .inp) is set to 1. Binary files are written at the time interval specified in the program control file (*.inp) by nskip. The files are named trimrout.nnn where nnn is the sequence number for the requested time interval. File contents are the same as the ASCII output file but omit the first 2 lines.

Time-Series Output File

The time-series file, tsdata.dat, contains the time series data requested in the program control file (file extension .inp). Results are written at the time interval specified in the program control file (file extension .inp) by ntsskip. This file is always named tsdata.dat.

File contents

Line number	Variables
1-maxstp/nskip	row, itsnodes(k,t),k=1,ntsdata

Variable definitions

row – the line number

itsnodes(k,t) – the requested variable for time step t at the kth grid location specified in the program control file

Binary Restart File

The binary (or unformatted) restart file, restart.dat, can be either an input file or an output file. It contains data that can be used to supply initial conditions to the program. Whether this file is written or used for initial conditions is specified in the program control file (file extension .inp) by the nrstrt variable.

ASCII Restart File

The ASCII restart file, rstij.dat, can either be an input or output file. It contains data that can be used to supply initial conditions to the program and is named rstij.dat. Whether this file is written or used for initial conditions is specified in the program control file (file extension .inp) by the nrstrt variable.

File contents

Line number	Variables
1-number of cells	i,j, eta(i,j), u(i,j), v(i,j)

Variable definitions

i – east-west grid index

j – north-south grid index

eta(i,j) – water-surface elevation, in meters, referenced to the vertical datum at cell i,j for the last time step

u(i,j)- averaged east-west velocity at cell i,j for the last time step

v(i,j) – averaged north-south velocity at cell i,j for the last time step